POLYMERIZATION AND POLYMER CHARACTERIZATION
OF
N-VINYLCAPROLACTAM


A THESIS SUBMITTED TO
THE GRADUATE SCHOOL OF NATURAL AND APPLIED SCIENCES
OF
MIDDLE EAST TECHNICAL UNIVERSITY


BY


ÖZLEM POLAT


IN PARTIAL FULFILMENT OF THE REQUIREMENTS
FOR
THE DEGREE OF MASTER OF SCIENCE
IN
POLYMER SCIENCE & TECHNOLOGY


SEPTEMBER 2005

Approval of the Graduate School of Natural and Applied Sciences

_____
Prof. Dr. Canan Özgen
Director

I certify that this thesis satisfies all the requirements as a thesis for the degree of Master of Science.

_____
Prof. Dr.Ali Usanmaz
Head of Department

This is to certify that we have read this thesis and that in our opinion it is fully adequate, in scope and quality, as a thesis for the degree of Master of Science.

_____
Prof. Dr. Ali Usanmaz
Supervisor

**Examining Committee Members**

Prof. Dr. Duygu Kısakürek    (METU,CHEM)    _____

Prof. Dr. Ali Usanmaz        (METU,CHEM)    _____

Prof. Dr. Zuhal Küçükyavuz   (METU,CHEM)    _____

Prof. Dr.Jale Hacaloğlu       (METU,CHEM)    _____

Asst.Prof. H. Nur Testereci   (Kırıkkale U,CHEM)    _____

**I hereby declare that all information in this document has been obtained and presented in accordance with academic rules and ethical conduct. I also declare that, as required by these rules and conduct, I have fully cited and referenced all material and results that are not original to this work.**

Name, Last name :

Signature :

**ABSTRACT**


POLYMERIZATION AND POLYMER CHARACTERIZATION
OF
N-VINLYCAPROLACTAM



Polat, Özlem

M.S., Department of Polymer Science and Technology

Supervisor : Prof. Dr. Ali Usanmaz


September 2005, 78 pages

In this study, N-vinylcaprolactam was polymerized by radiation in the solid state. The polymerization was carried out at room temperature under vacuum and open to atmosphere respectively. The polymerization mechanism showed autoacceleration and the rate of polymerization was higher in the presence of oxygen. However the limiting conversion was 100% under vacuum conditions and 90% in the present of oxygen. This is due to the low molecular weight oligomer formation in the presence of oxygen. The polymers were characterized by FT-IR, NMR, DSC, TGA, Light Scattering, GPC, Viscosity, X-Ray and mass spectrometry methods. FT-IR and NMR results showed that polymerization proceded through the vinyl groups and caprolactam is a pendent group. DSC results show that the polymer produced could be polymerized further or crosslink by heat treatment. The $T_g$ value for the polymer obtained from radiation induced polymerization was about 147 $^0$C. It increased to 174 $^0$C after thermal treatment. Solution properties were studied by Light Scattering , GPC and viscosity measurements. The solution behavior of the polymer was highly dependent on the molecular weight of the polymer. This effect was also the

conformation of polymer in solution and the viscosity properties. Since the polymer obtained had low molecular weight a regular relation could not be obtained for the radius of gyration, hydrodynamic radius and viscosity. X-ray diffraction studies showed that the monomer structure was retained up to about 86% conversion of monomer to polymer. The chain structure of the polymer was confirmed further by mass spectroscopic results.

# ÖZ

## N-VİNİLKAPROLAKTAM POLİMERLEŞTİRİLMESİ
## VE
## POLİMER KARAKTERİZASYONU

Polat, Özlem

Yüksek Lisans, Polimer Bilimi ve Teknolojisi Bölümü

Tez Yöneticisi : Prof. Dr. Ali Usanmaz

Eylül 2005, 78 sayfa

Bu çalışmada, N-vinylcaprolactamın katı hal polimerizasyonu radyasyon ile gerçekleştirilmiştir. Polimerleşme tepkimesi, açık havada ve vakum altında oda sıcaklığında yapılmıştır. Polimerleşme kendi kendine hızlanan bir mekanizma takip etmektedir. Polimerleşme hızı oksijenli ortamda daha yüksektir. Vacum altında polimerleşmeye limit dönüşüm %100, oksijenli ortamda ise %90'dır. Ancak oksijenli ortamda düşük molekül ağırlıklı oligomerler oluşmaktadır. Elde edilen polimer örnekleri FT-IR, NMR, DSC, TGA, Light Scattering, GPC, Viscosity, X-Ray ve Mass spektroskopik methodları ile karakterize edilmiştir. FT-IR ve NMR sonuçları polimerleşme mekanizmasının kaprolaktam yan grup bağlı vinil grupları üzerinden yürüdüğünü göstermektedir. DSC sonuçları ise ısı ile muamele sonucu polimerizasyonun devam ettiğini veya çapraz bağların oluştuğunu göstermektedir. Radyasyonla polimerleştirme sonucu elde edilen $T_g$ değeri yaklaşık $147^0C$ iken, polimerin ısı ile etkileşimi sonucunda $T_g$ yaklaşık $174^0C$ye çıkmaktadır. Ayrıca çözelti özellikleri, Light Scattering , GPC ve viskozite ölçümleriyle incelenmiştir.

Çözelti davranışlarının molekül ağırlığına önemli ölçüde bağımlı olduğu ve polimerin konformasyonunun değiştiği saptanmıştır. Bunun sonucu olarak viskozite ölçümleri molekül ağırlığına bağlı olarak düzenli değişen değerler vermemektedir. Elde edilen düşük molekül ağırlıklı polimerlerde molekül ağırlığı ile yumaklaşma yarıçapı ( radius of gyration), hidrodinamik yarıçapı (hydrodynamic radius) ve viskosite arasında düzenli bir ilişki görülmemiştir. X-Işın çalışmaları, monomerin polimerleşmenin %86 oluncaya kadar yapısını koruduğunu ancak bu dönüşümden sonra monomer yapısının bozulduğunu göstermiştir. Kütle spektroskopik (Mass) çalışmaları ise elde edilen polimer zincir yapısını onaylamaktadır.

Anahtar Kelimeler: Katı hal polimerleşmesi, N-Vinylkaprolaktam, radyasyonla polimerleşme, karakterizasyon.

**TO THE MEMORY OF MY FATHER**

# ACKNOWLEDGMENTS

I express my sincere appreciation to Prof. Dr. Ali Usanmaz for his guidance throughout this study.

I would like to thank to Prof. Dr. Jale Hacaloğlu for her kindness help.

I wish to thank for the significant contributions of Leyla Molu who helped during GPC and Light Scattering measurements. Thanks go to my friend Emir Argın for her moral support and helps.

And my deep thanks are to my mother and my brothers for their understanding, encouragement and patience.

# TABLE OF CONTENTS

# LIST OF TABLES

TABLES

# LIST OF FIGURES

# CHAPTER I

# INTRODUCTION

## 1.1. Radiation Induced Solid-State Polymerization

The polymerization by radiation can be initiated either by a radical or an ion. Although radiation produces ions and excited molecules as a primary act, most of the polymerization reactions already studied have been found to proceed by a radical mechanism (1).

The advantages of the radiation induced polymerization are as follows:

1. Some monomers that are difficult to polymerize by conventional methods can be polymerized by radiation.
2. Penetrating radiation, in particular gamma radiation, ensures regular initiation throughout the bulk of the solid monomer.
3. The polymers of high purity, containing no residues of initiators, catalysts, etc can be obtained by radiation initiation.
4. It is possible to carry out polymerization "on site" for manufacturing polymer as parts in the hard-to-reach places (2).

The solid state polymerization was reported for the first time by Schmitz and Lawton in 1951(3). Adler et al. (4) found that acrylamide could be polymerized in the solid state by radiation. It was expected that a well-oriented crystalline polymer would be obtained after polymerization due to limited mobility of molecules in solid matrix. However, resulting polymer was amorphous. This drew attention of scientist to the study of the effect of crystal structure on solid state polymerization (5).In 1956 Restaino et al. published data on the gamma radiation-induced polymerization of a wide range of solid monomers, including acrylic acid and its barium, calcium and potassium salts which only melt at high temperatures. Lawton, Grubb and Baldwit

1

(1956) polymerized a cyclic siloxane (hexamethylcyclotrisiloxane) in the solid state by electron irradiation. Radiation induced polymerization of acrylonitrile ( between -83° C and -196 °C) in solid state has been carried out around melting point of the monomer (6). The rate of polymerization of solid acrylonitrile was 30 to 40 times faster than that in the liquid state. Polymer yield was higher for monomers recrystallized by slow cooling. Because, slow cooling leads to the formation of large and well oriented monomer crystallites. Polymerization of potassium acrylate in crystalline state was reported by Morewetz and Rubin (7) at -78 C using Gamma-Rays. Morawetz (8) showed that there is no clear correlation between solid-state polymerization induced thermally and by radiation (9). Adler and Reams (10) indicated that the polymerization would proceed at the interphase between monomer and polymer of acrylamide after some polymer formed. It was supported by an experiment in which acrylamide single crystal was divided into two parts, one part was wrapped with aluminum foil, and other part was exposed to gamma radiation. After some time, the sample photographed under polarized microscope. In the photograph, the side polymerized was black, while other part was bright. Two sides were clearly different from each other. So, Adler believed that the crystal structure of acrylamide molecules exerted no influence on the polymerization because polymerization proceeded at the interphase between monomer and polymer. Adler et al.(11) explained that the reason for the formation of amorphous acrylamide polymer, was due to the structure of monomer; the –C=C double bond (1.34 A°) opened and the transformed to –C-C- single bonds (1.54 A°) during polymerization. However, intermolecular distance between molecules decreased from Van der Walls distance of about 3.75 A° to 1.54 A°, C-C single bond length. When both changes combined, overall volume of the system was decreased about 12%. That volume reduction created a strain in the crystal lattice. Therefore, the crystal structure broke down and caused the polymer to be amorphous. The crystal structure effect and mechanism of radiation induced solid state polymerization of acrylamide was well documented by Usanmaz (12).

Eastmond et al.(13) found that when acrylic acid polymerization was initiated with polarized UV radiation, the rate of polymerization in the initial stage showed strong dependence on the angle between the plane of electric vector of radiation and crystallographic axes, i.e. the rate of polymerization is maximum when electric vector of radiation is parallel to a crystallographic axis. They suggested that this feature was in accordance with other showing that absorption of radiation by vinyl groups was ultimately responsible for radical formation. These facts indicate that the molecular disposition has an important influence on the initial stage of polymerization. However, in the crystal lattice , dimmers of acrylic acid are further from each other than the possible interaction which has intermolecular vinyl C….C distance of 3.52 A°. Therefore, all molecules have to be rearranged to be able for combination of monomer molecules. The chain propagation is isotropic due to large movements. The resulting polymer is atactic and amorphous. In general, vinyl polymers can not be crystallized except a few cases, such as poly (vinylalcohol) (14), poly (vinylchloride) (15), poly (vinylflouride) (16) . Atactic poly (vinylalcohol) is highly crystalline, because hydrogen bonds are formed and stabilize the crystal lattice even though the polymer chain is atactic. Fluorine atoms in poly (vinylfluoride) are small enough to permit polymer crystallization, with short syndiotactic-predominant sequences. In vinyl separate polymer, crystal structure is formed from side chains in the form of layers. The distance between layers are 25.4 A°. So, polymer enchainment occurred along these layers and crystal structure of polymer didn't disrupt (8). This serves to yield crystalline polymer. Okamura and his associates demonstrated that the structure of monomer lattice imposes an orientation on polymers obtained by γ-irradiation of trioxane, β-propilactone, diketene. In the case of polyoxymetylene obtained obtained by post polymerization irradiated large crystals of trioxane (17) , β-propilactone (18), diketene (19). In the case of polyoxymetylene obtained obtained by post the polymerization irradiated large crystals of trioxane, the polymer was found to be highly ordered not only with respect to the orientation of the fiber axis, but also in the manner in which the polymer chains packed, so that the material resembled in a large single crystal.

3

A typical example of lattice control polymerization can be seen in four center type of polymerization of 2, 5-distyrlpyrazine studied by Hasegawa and Suzuki (20). Distyrlpyrazine has two crystalline modifications; plate like crystals which are orthorhombic and needle like crystals which are monoclinic. Plate-like crystals undergo prompt photopolymerization in the crystalline state under influence of UV light or sunlight into high molecular weight crystalline polymer. However, needle like crystals do not undergo any change with irradiation. Van der Waals distance of plate like crystals is lower than 4 A°. So polymerization takes place with slight rotations and translations. Therefore crystal structure of monomer is protected. This type of polymerization is topotactic.

Usanmaz and Melad (21) polymerized 3-aminocrotonamide by radiation in solid state. Polymerization occurred by a condensation process with evolution of $(2n-1)NH_3$ molecules for each $2n$ monomer molecules. The polymer formed was similar in crystal structure to that of monomer. Thus, it gives a topotactic polymerization by condensation. Structure and properties of polurethane and acrylate prepolymer films, obtained by electron beam (EB) and UV, in solid state polymerization examined to reveal the characteristic of these radiation polymerizations (22). Although polyurethane and acrylate films from EB and UV solid state polymerizations mainly consisted of amorphous and crystalline phases, it was proved that the film obtained by 10 Mrad of EB radiations at 25°C had higher crystallinity and larger crystallite size than film from UV irradiation. This is assumed to be due to the reason that EB irradiation below melting point of polyurethane-acrylate can lead to crosslinking without the destruction of original crystal structure. On the other hand, the UV polymerization proceeded around melting point of crystalline structure by absorbing electromagnetic radiation other than the UV absorbed by a photoinitiator.

The mechanism of polymerization is greatly influenced by monomer crystal geometry in the solid state. The change in the crystal structure most probably orients the molecules in more favorable arrangements for polymerization of allythiourea

(23). Leading to a higher maximum conversion. When IR spectrum of partially polymerized monomer was investigated, it was seen that, although monomer peaks were partially covered by broad amorphous polymer peak, the monomer molecules still retained their crystalline structure at 46% conversion. The changes in relative intensities of monomer peaks during polymerization were most probably due to distortion of crystal morphology. The polymer was amorphous and isotropic; it always looked dark between crossed polarizer, where the monomer was anisotropic and looked bright except at extinction positions in polarizing microscope. The results proved that polymerization did not proceed by a two phase mechanism like the monomer-polymer interphase polymerization. The effect of oxygen on the polymerization of allylthiourea was investigated by Usanmaz and Yılmaz (23). The accelerating effect of oxygen was clear at conversions above 40%. This suggests that the crystal structure becomes distorted with the formation of polymer to allow easier diffusion of oxygen.

## 1.2. Mechanism of Free Radical Solid State Polymerization

The polymerization involves initiation, propagation and termination:

**Initiation:**

The first step is the activation of a monomer molecule to form a free radical.

$$M \xrightarrow{k_i} R\cdot$$
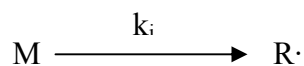
Catalyst, if present, will be activated to give radicals.

$$Cat \xrightarrow{k_d} 2R\cdot$$

$$R_i = 2\, fk_i[Cat] = 2\, f\, k_i\, I$$

5
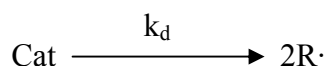
Where f is the efficiency factor and $k_i$ is the initiation rate constant.

**Propagation:**

A free radical adds on to a double bond of a monomer molecule, thereby regenerating another free radical etc.

$$R \cdot + M \xrightarrow{k_p} RM \cdot$$

..............................

..............................

$$RM_n \cdot + M \xrightarrow{k_p} RM_{n+1} \cdot$$
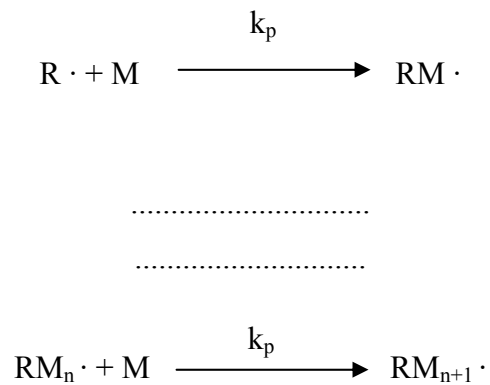
Where R is a primary radical, M is the monomer and $RM_n$ is a growing polymer chain. The propagation rate equation used in conventional homogenous polymer kinetics.

$$-d[M] / dt = k_p [M] [R]$$

where kp is the propagation rate constant, [M] is the monomer concentration and [R] is the total concentration of radical.

**Termination:**

The termination step involves the mutual annilation of two radicals. This can take place in two chains may terminate by combination.

$$RM_n \cdot + RM_m \cdot \xrightarrow{\ k_{tc}\ } P_{n+m}$$

Or they may undergo disproportionation with the transfer of a hydrogen atom and the formation of an unsaturated end group.

$$RM_n + RM_m \xrightarrow{\ k_{td}\ } P_n\text{-}CH_2\text{-}CH_3 \ + \ P_m\text{-}CH=CH_2$$

The rate equation will be:

$$R_t = (k_{tc} \ + \ k_{td}\,)\,[\,R\,]^2 = k_t\,[R]^2$$

Usually a steady state concentration of [R] is assumed at low conversions where the rate of initiation and termination are equal:

$$R_i = \ R_t$$
$$2\,f\,k_i\,I = k_t\,[R]^2 \quad \text{where } k_t = k_{tc} \ + \ k_{td}$$

The radical concentration will be:

$$[R] \ = (2fk_iI\,/\,k_t\,)^{1/2}$$

Then the propagation rate is:

$$-d[M]/dt = kp[M](\,2\,f\,k_i\,I\,/\,k_t)^{1/2}$$

Thus, the integrated rate equation will be:

$$\log([Mo]/[M]) = kp.(k_i.f.I/k_t)^{1/2}\,t/4.606 = k\,I^{1/2}\,t$$

where I is a constant for any one series of experiments and Mo is initial concentration of the monomer. Then a plot of log [Mo/M] versus t should give a straight line with the slope of k

7

## 1.3 POLY (N-VINYLCAPROLACTAM)

N-Vinylcaprolactam, NVCL, monomer contains (24) hyrophilic cylic amide (caprolactam) attached to vinyl group by nitrogen. In the case of addition polymerization, the vinyl group is used for polymerization and caprolactam becomes pendent group. Thus, the polymer backbond is a vinyl type polymer. The presence of side lactam group makes the polymer very valuable for bioapplication. If the condensation polymerization is carried out, the caprolactam ring is opened and nylon type polymer is obtained. The side group in this polymer chain will be vinyl group. Then, the polymer can be used as an engineering polymer. After applications such as drawing into fiber, the side vinyl group can be used for crosslinking to improve the mechanical strength of polymer.

The crystal structure of monomer is reported by Tishchenko et al. (25). The compound is water soluble with a low critical temperature of 36-37 $^0$C. The crystals are triclinic of cell parameters: a = 8.170(4) A°, b = 8.094(4) A°, c = 6.799(4) A°, $\alpha$ = 99.92(1)$^0$, $\beta$ = 88.89(1)$^0$, $\gamma$ = 115.30(1)$^0$. Space group is P$\bar{1}$. The molecule exhibits a chair conformation and the amide and vinyl groups are approximately coplanar. The charge distribution calculated (26) indicates the increase reactivity of the terminal C atom (CH$_2$= ) in vinyl group, which promotes the polymerization reaction given polymer chain as follows:
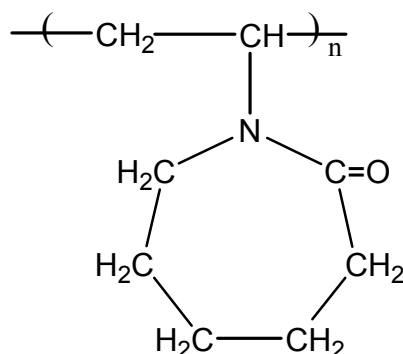
The kinetic of N-vinylcaprolactam polymerization has not been reported in literature. However, due to the interesting and unique solution properties, the solution properties have been studied intensively. In polymer chain (PVCL), nitrogen is directly attached to the hydrophobic carbon-carbon backbone chain (27). Therefore, the hydrolysis of PVCL does not produce low molecular weight amines (28). The appropriate balance of hydrophobicity and hydrophilicity in the polymer chain is responsible for unusual properties of polymer. Cheng et al. (29) reported the polymerization of NVCL by radiation in water. The effects of radiation dose and total dose on the viscosity of polymer obtained and low critical solution temperature were studied. They showed that the polymer obtained with radiation of 2-14 Gy/min and total radiation a little larger then 2 kGy has good temperature sensitivity and uniformity. Lozinsky et al (30) reported the polymerization of NVCL by emulsion polymerization using water as solvent and ammonium persulphate/ tertiary amine redox initiator. They have studied the molecular weight and molecular weight distribution, their temperature-dependent solution behaviors and the thermodynamic parameters of phase segregation process of polymer using SEC, DSC. Gao et al (31) reported narrowly distributed spherical poly(N-vinylcaprolactam) (PVCL) microgels prepared by precipitation polymerization in water using potassium persulpate/ tertiary amine redox initiator. The effect of both anionic (sodium dodecyl sulfate, SDS) and cationic (N-dodecylpyridinium bromide, DPB) surfactants on the swelling and shrinking of the microgels were investigated by laser light scattering (LLS). They showed that the microgels gradually shrank to the collapsed state when the temperature increased from 20 to approx. 38°C. The addition of anionic surfactant caused an extra swelling of the microgels and shifted the collapsing temperature higher, whereas the addition of cationic surfactant has different effects on the swelling and shrinking of the microgels prepared by using different initiators, depending on whether the decomposed fragments of the initiator are ionic or neutral.

PVCL is one of the several nonionic synthetic polymer soluble in water and exhibit thermosensitive properties in an aqueous solution (32), Peng (33), Ivanov (34), Lozinsky (30). The relation of temperature-solubility of PVCL was first

reported in 1968 (35). When the aqueous solutions are heated, phase separations are observed in the range of 32-38 °C (36); a low temperature transition (lower critical solution temperature, LCST) at 32°C is attributed to a micro segregation of hydrophobic domains and a higher temperature transition around 38°C, corresponding to the gel volume collapse itself. Therefore, this polymer is considered to be suitable materials for novel biotechnological applications such as in drug delivery, bioseparation, diagnostics, etc. (29).

The radiation graft polymerization of *N*-vinylcaprolactam onto polypropylene films was studied by Kudryavtsev et al. (37). The radiation graft polymerization was performed with preirradiation in air (peroxide method) or using a direct method in aqueous solutions and organic solvents. The effects of radiation dose, reaction time, monomer concentration, and homopolymerization inhibitor on the radiation graft polymerization were studied. They showed by DSC and equilibrium swelling in water that the modified polymers of polypropylene with grafted poly( N-vinylcaprolactam) chains exhibited thermoresponsive properties.

Kirsh and Yanul (26) studied structural transformations and water associate interactions in poly-N-vinylcaprolactam-water system. They showed that (i) the conformation type of a side seven-member ring deduced by quantum-chemical calculations is the chair; (ii) the main chain of PVCL prepared by usual radical polymerization has syndiotactic structure; (iii) the calculation of charge distribution on a C=O oxygen atom in the analogue of PVCL chain link gives the large electron density value being -0.362, (iv) the addition of water to PVCL changes $T_g$ from 147°C (dry polymer) to -17°/ -38°C at N (number of water molecules per unit) being 2.6/8.0.

Dynamic light scattering measurements have been performed for aqueous solutions of thermosensitive linear poly(*N*-vinylcaprolactam) (PVCL) macromolecules in the presence of NaCl and different water soluble amphiphilic organic compounds: pyrogallol (neutral amphiphilic compound), cetylpyridinium

chloride (cationic surfactant) and sodium dodecylsulfate (anionic surfactant) (31) (38). A decrease in the macromolecular hydrodynamic diameter is observed upon addition of ionic surfactants (SDS, CPC) at low surfactant concentrations. (39) Lebedev et al. (40) reported the results obtained by SANS and NSE around the coil-globule transition (tc=32˚C) temperature. The increase of temperature causes the collapse of coils.

## 1.4. MOLECULAR WEIGHT DETERMINATION

The molecular weight of polymers were measured by viscosity, light scattering and GPC methods.

### 1.4.1. Viscosity Measurement

In viscosity method, the flow-time for a defined volume of solvent and solution are compared and their ratios are taken. If the flow time for the solvent is $t_0$ and that of solution is t, then the relative viscosity, $\eta_r$, is

$$\eta_r = \frac{t}{t_0}$$

the specific viscosity, $\eta_{sp}$, in terms of $\eta_r$

$$\eta_{sp} = \eta_r - 1 = \frac{t - t_0}{t_0}$$

The viscosity data as a function of concentration are extrapolated to infinite dilution by means of the Huggins or Kraemer equation.

$$\frac{\eta_{sp}}{c} = [\eta] + k^{'}[\eta]^2 c \qquad \text{(Huggins, 1942)}$$

$$\frac{\ln \eta_r}{c} = [\eta] + k^{''}[\eta]^2 c \qquad \text{(Kraemer, 1938)}$$

The viscosity molecular weight relation is:

$$[\eta] = KM^a \quad \text{and} \quad \log[\eta] = \log K + a \log M$$

If the K and a values are found from GPC or light scattering methods, the molecular weight can be determined from viscosity measurements.

## 1.4.2. Light Scattering Measurement

The measurement of weight average molecular weight, $M_w$ by Light Scattering is a widely used technique. It is based on the optical heterogeneity of polymer solutions.

The fundamental relationship for light scattering is given as

$$\frac{Kc}{R(\theta)} = \frac{1}{\overline{M}_w P(\theta)} + 2A_2 c + ...$$

K is as follows:

$$K = \frac{2\pi^2 n_o^2}{N_A \lambda^4}\left(\frac{dn}{dc}\right)^2$$

where $n_0$ is the refractive index of the pure solvent; dn/dc the specific refractive increment of the dilute polymer solution and $\lambda$ the wavelength of the incident light. The term $R(\theta)$ is called *Rayleigh ratio,* which is defined as

$$R(\theta) = \frac{i(\theta)r^2}{I_0 V}$$

where $I_0$ is the intensity of the incident light beam and $i(\theta)$ is the intensity of the scattered light.

In the Zimm Method a double extrapolation to both zero concentration and zero angle is used to obtain information concerning molecular weight, second-virial coefficient ($A_2$), and chain dimensions. In the limit of small angles where $P(\theta)$ approaches unity than the equation becomes

$$\frac{Kc}{R(\theta)} = \frac{1}{\overline{Mw}}\left[1 + \frac{16}{3}\left(\frac{\pi n}{\lambda}\right)^2 <s^2> \sin^2\left(\frac{\theta}{2}\right)\right] + 2A_2c$$

where, K is the optical constant, c is the concentration, $A_2$ is the second virial coefficient, $<s^2>$ is radius of gyration and $\lambda$ is the wavelength of the incident beam in the solution. The $Kc/R(\theta)$ versus $<s^2>\sin^2(\theta/2)+kc$, where k is an arbitrary constant that is added to provide spacing between each curve, and a double extrapolation to $\theta = 0^0$ and c = 0 gives Mw as the reciprocal of the intercept. $A_2$ can then be determined as one-half of the slope of the extrapolated line at $\theta = 0^0$; the mean-square radius of gyration is obtained from the initiall slope of the extrapolated line at c = 0 as

$$<s^2> = \frac{3\overline{M}_w}{16}\left(\frac{\lambda}{\pi n}\right)^2 \times \text{slope} \ (\text{at} \ \theta = 0)$$

The measurements of radius of gyration, $R_g$, hydrodynamic radius, $R_h$ and diffusion coefficient, D gives the information about the solution properties and conformation of polymer chain in solution.

### 1.4.3. Gel Permeation Chromatography

Gel Permeation Chromatography, sometimes also called size exclusion chromatography, SEC, is a separation method for higher polymers. GPC is widely used method for estimating molecular weight and its distributions. The technique is much more rapid and convenient, giving reliable and reproducible chromatograms and is widely used for routine polymer characterization and in quality control areas.

This method is capable of determining the entire molecular-weight distribution of a polymer sample from which all molecular weight averages – number average ($M_n$), weight average ($M_w$), and z average ($M_z$) and also polydispersity ($M_w/M_n$) can be determined. The separation takes place in a chromatographic column filled with beads of a rigid porous gel, highly crosslinked porous polystyrene and porous glass are preferred as column-packing materials. The pores in these gels are of the same size as the dimensions of polymer molecules.

A sample of a dilute polymer solution is introduced into a solvent flowing through the column. As the dissolved polymer molecules flow through the porous beads, they can diffuse into the internal gel to an extent depending on their size and the pore-size distribution of the gel. Larger molecules enter only a small fraction of the internal portion of the gel, so, it spends less time inside the gel and it flows sooner through the column. In contrast smaller molecules penetrate more and flow later through the column. By this way, the different molecular species are eluted from the column in order of their molecular size as distinguished from their molecular weight.

The concentration of polymer molecules in each eluting fraction can be monitored by means of a polymer-sensitive detector, such as refractive, infrared or ultraviolet.

The universal calibration curve is based on the proportionality of the product [η]M to the hydrodynamic volume of a polymer molecule in solution. In calculation of molecular-weight averages, the signal strength (peak height) is proportional to $W_i$ and if a proper calibration curve is available to relate Vi to the molecular weight ($M_i$) of the calibration standard, the direct calculation of all molecular weights and polydispersities can be available.

## 1.5. X-Ray

Information of polymer obtained from X-ray diffraction photograph as follows:

- Identification of polymers
- Determination of the identify period
- Lateral ordering of polymeric chains
- Orientation of crystallites
- Crystalline size
- Crystalline content
- Unit cell data
- Determination of the point group
- Atomic positions within the unit cell

In order to index the powder x-ray pattern of a sample crystallized in triclinic unit cell, the following equation is used.

$$d^{*2} = a^{*2}h^2 + b^{*2}k^2 + c^{*2}l^2 + 2hka^*b^*hk\cos\gamma^* + 2hla^*c^*\cos\beta^* + 2klb^*c^*\cos\alpha^*$$

where hkl are Miller indices, $a^*$, $b^*$, $c^*$ are reciprocal cell edges and $\alpha^*$, $\beta^*$, $\gamma^*$ reciprocal cell angles. If cell parameters are known the theoretical $d^{*2}$ are calculated for different hkl combination and compared to the experimentally calculated values:

$$d^{*2} = (2\sin\theta/\lambda)^2$$

where $\lambda$ is x-ray wavelength and $\theta$ is Bragg reflection angle. In this study , the powder pattern of monomer and monomer- polymer mixtures after the radiation were

recorded to observed the changes in crystal structure of monomer during polymerization. The indexing of diffraction of data were done by using the reported cell parameter data given in literature (41).

## 1.6. Pyrolysis Mass Spectrometry

Pyrolysis is the thermal degradation of complex material in an inert atmosphere or vacuum. It causes molecules to cleave at their weakest points to produce smaller, volatile fragments called pyrolysate (42). Pyrolysis-mass spectrometry (Py-MS) is a very fast and sensitive fingerprinting technique. Using this method, the sample is placed in high vacuum and heated under controlled conditions. The organic material undergoes rapid decomposition and the low molecular weight products enter into a mass spectrometric device, where the pyrolysate is quantified (43). Since pyrolysis mass spectrometry techniques are carried out under high vacuum conditions, the possibility of secondary reactions is minimized (44). Pyrolysis mass spectrometry techniques can be used to determine not only the thermal behavior and decomposition products but also to investigate the structure of the polymers (45).

Among the various pyrolysis mass spectrometry techniques direct pyrolysis mass spectrometry technique allows the thermal decomposition products of the polymer sample to be observed directly in the ion source of the mass spectrometer, so that the evolving products are ionized and continuously detected by repetitive mass scans almost simultaneously with their formation. Since pyrolysis is accomplished under high vacuum, the thermal degradation fragments are removed from the hot zone, thus molecular collisions have low probability the generation of secondary reactions is reduced (46). It is a simple and quick method for structural and thermal characterization of polymers .

## 1.7. Aim of the Work

In this work N-vinylcaprolactam will be polymerized in solid state by radiation. The polymerization will be carried out in vacuum and open to atmosphere conditions to observe the effect of oxygen on polymerization mechanism. The kinetic of polymerization will be investigated. Polymer obtained will be characterized by spectroscopic, thermal methods and X-Ray diffraction. Molecular weight determination by Light scattering, GPC and viscosity methods will give information about the solution properties of polymer. The molecular structure of polymer will be investigated by FT-IR, NMR and Mass spectroscopy. The thermal properties of monomer and polymer will be studied using the DSC. The crystal structure effect on solid state polymerization of N-vinylcaprolactam will be investigated by XRD method.

# CHAPTER II

# EXPERIMENTAL

## 2.1 CHEMICALS

N-Vinylcaprolactam: It was obtained from Aldrich. It was purified by recrystallization in hexan.

Diethylether: Technical grade diethylether obtained from Riedel de-Haen.

Benzen: It was product of Baker Analyzed.

Deionised water was used in experiments.

## 2.2 INSTRUMENTATION

### 2.2.1 Polymerization Tubes

The tubes were 11 mm in diameter and 10 cm in length Pyrex tubes.

### 2.2.2 High Vacuum System

High vacuum system was used to evacuate the irradiation tubes in which the solid monomer was present, down to $10^{-4}$ -$10^{-5}$ mmHg pressures.It was composed of the following parts.

**a) Duo-Seal Vacuum Pump**

It is a product of "Sargent-Welch  Scientific Co." Model 1399 and capable of pressure reduction down to $1.5 \times 10^{-2}$ mmHg

**b) Mercury Diffusion Pump**

It is a water-cooled one-stage diffusion pump with an approximate capacity of 200 ml of mercury. Mercury was heated by a 143 W metallic bond resistive heater operating at 130 V, which is a product of "Pliz Co." Type 62.

**c) Main Manifold**

It was made up of a pyrex glass tube with diameter of  4.53 cm. and length of 110 cm. carriying one outlet tube with high vacuum stockcock for the connection of irradiation tube.

**d) Liquid Nitrogen Traps**

Irradiation tube was connected a trap through a high vacuum stopcock. To protect the pumbs from the chemicals evaporated at low pressures, two pyrex traps were used. One of the traps was connected between the mercury diffusion pump and the other was connected between the main and mercury diffusion pump.

**2.2.3 Radiation Source**

For the irradiation of sample by gama rays Gamma cell 220 (Atomic Energy of Canada Ltd. Co.) The dose rate of the radiation source was about 13 krad/h.

### 2.2.3 Viscometer

Schott Gerate AVS 400 model automatic viscometer equipped with Schott CT 1150 model thermostat was used to determine the viscosity of the polymers.

### 2.2.4 Infrared Spectrometer

Infrared Spectra of monomer and polymers obtained from KBr pellets by using Perkin Elmer Spectrum-One FT-IR Spectrometer.

### 2.2.5 Differrential Scanning Calorimetry

The thermal analyses of the samples were recorded by TA-DSC 910 S differential scanning calorimeter. Heating rate was $10°C/min$. From $-50°C$ to $300°C$ under nitrogen gas atmosphere.

### 2.2.6 Thermogravimetric Anaysis (TGA)

Thermal stability of PVCL was characterized by Dupont 951 Thermogravimetric Analyzer. Thermograms were recorded under $N_2$ atmosphere in a temperature range of $30°C$ to $900°C$ with $5°C/min$ heating rate.

### 2.2.7 Nuclear Magnetic Resonance

The molecular structure of PVCL was determined by using Magnetic Resonance Spectrometer, Ultrashield 400 MHz Digital NMR Bruker, with $^1H$ and $^{13}C$ Spectrometers.

**2.2.8 Light Scattering**

Molecular weight determination of poly(vinylcaprolactam) was found by light scattering method. The plots were obtained by using the Malvern CGS-3 System .

**2.2.9 Gel Permation Chromatography**

Molecular weight distributions were measured by size exclusion chromatography (SEC) on a PL-GPC 220 integrated GPC system.

**2.2.10 X-Ray Powder Diffractometer**

X-Ray powder diffraction patterns (XRD) were taken by using Rigaku Miniflex with Cu (K$\alpha$ 30 kV, 15 mA, $\lambda$=1,54178 A$^{o}$) radiation.

**2.2.11 Mass Spectrometer**

Direct insertion probe pyrolysis mass spectrometry (DIP-MS) system consists of a 5973 HP quadrupole mass spectrometer coupled to a JHP SIS direct insertion probe. This system provides fast scanning, self-tuning of experimental parameters and wide mass range. Mass spectra of the products was recorded at a scan rate of 2 scan/s in the mass range of 10-800 amu.

**2.3 Procedure**

**2.3.1 Radiation Induced Solid State Polymerization of N-Vinylcaprolactam**

The solid state polymerization of N-vinylcaprolactam initiated by Co-60 $\gamma$ rays was carried out under vacuum and in atmospheric air at room temperature.

About 3-5 g of monomer sample was put into the irradiation tube made up of pyrex glass and connected to the high vacuum system, evacuated at $10^{-4}$-$10^{-5}$ torr for about 4-5 hours with several times degassing. At the end of the evacuation; the tube was sealed and they were irradiated by γ rays for desired period of time at room temperature. For the polymerization in open air, similar amount of samples were placed in the tubes and put into irradiation source without evacuation.

After the irradiation, the tubes were break open, the irradiated samples were dissolved in a small amount of benzen and the polymer precipated in diethylether. The polymer was filtered and dried to constant weight. The percent conversion of the monomer to the polymer was calculated gravimetrically.

# CHAPTER III

# RESULT AND DISCUSSION

## 3.1 SOLID STATE POLYMERIZATION OF N-VINYLCAPROLACTAM

The radiation induced solid state polymerization of N-vinylcaprolactam gave gel type white polymer soluble in water and common organic solvents. The polymer is very hygroscopic and absorb water in air. The percent polymerization values agains time for the polymerizatiom under vacuum at room temperature, is plotted in Figure 3.1 and the results tabulated in Table 3.1. The polymerization curve showed a S-type behaviour. The initial rate is almost linear up to 10-12 %, then increases to high rate showing an auto accelaritation mechanism. The polymerization limited at 100% conversion. The percent conversion against time plot for polymerization in open atmosphere and at room temperature is shown in Figure 3.2 and the results are tabulated in Table 3.2. The initial rate of polymerization is much higher for polymerization in open atmosphere conditions compared to polymerization under vacuum. When the viscosity for different polymerization conditions are compared, it was observed that the moleculer weights of polymer are much lower for the polymerization in open atmosphere conditions. Therefore, the polymer obtained in open atmosphere conditions were soluble in ether also. The seperation of polymer from monomer was very difficult. The percent polymer could not be safely obtained for lower conversions in open atmosphere polymerization. However, the auto accelaration behaviour is not observed and the limiting conversion is about 90% in open atmosphere polymerization.The initial rate is linear up to about 70% conversion. Around the limiting coversion the data scattering is also higher in this case. This is again due to the termination of polymer chains in the presence of oxygen. The low molecular weight (tellomers and oligomers) polymers can not be seperated by precipitation method.

**Table 3.1  The % conversion vs. time results for solid state polymerization of N-vinylcaprolactam in vacuum at room temperature.**

| Time(hour) | % conversion | Viscosity(dL/g) |
|:---:|:---:|:---:|
| 45 | 1 | ………….. |
| 95 | 6 | …………. |
| 140 | 10 | 0,1225 |
| 160 | 11 | 0,1808 |
| 185 | 19 | 0,213 |
| 205 | 33 | 0,16125 |
| 210 | 50 | 0,2568 |
| 280 | 68 | 0,1945 |
| 305 | 86 | 0,1275 |
| 430 | 96 | 0,1769 |
| 500 | 81 | 0,1821 |
| 675 | 94 | 0,1800 |
| 840 | 100 | 0,0558 |
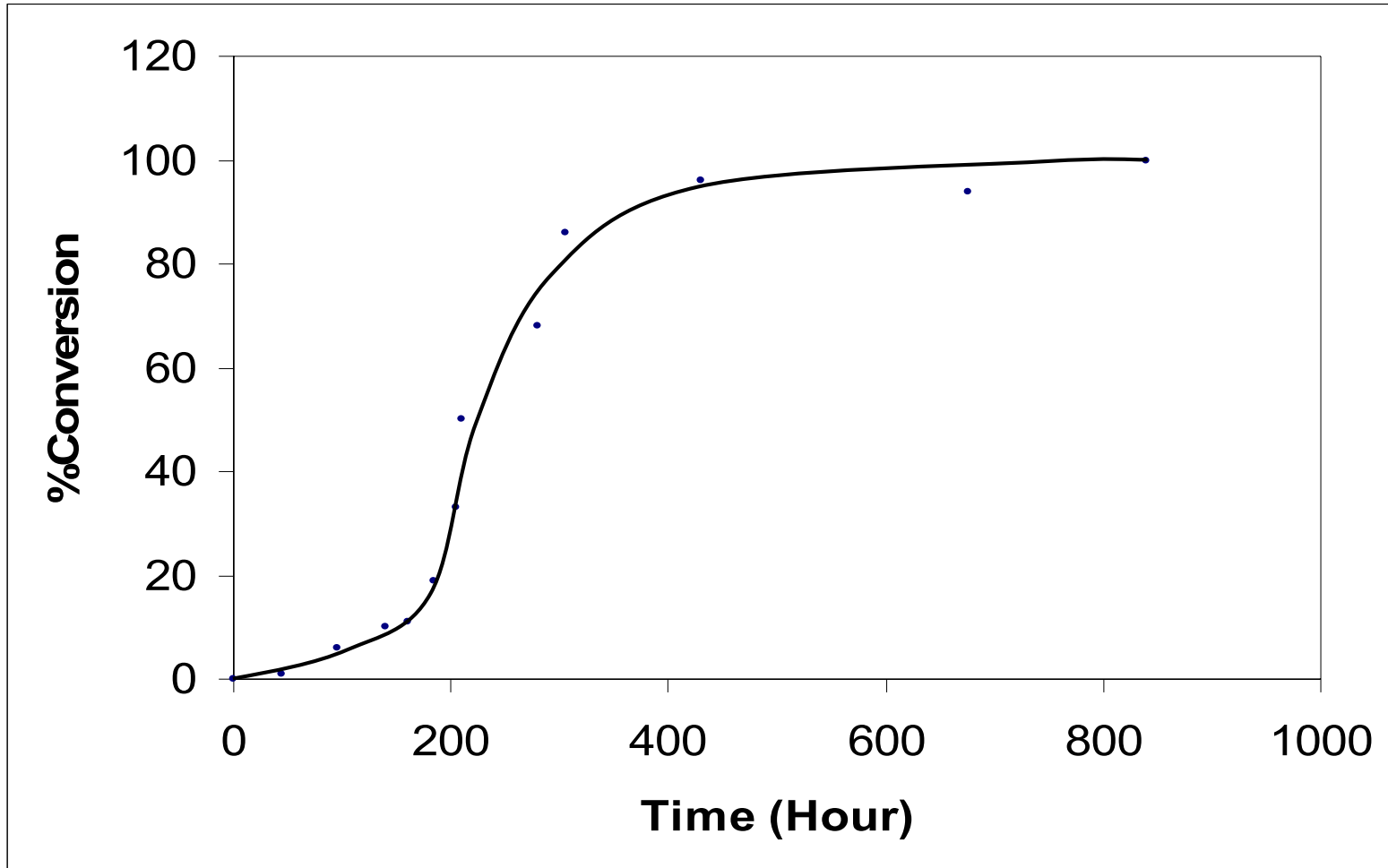
**Figure 3.1 % conversion vs time graph for solid state polymerization PVCL in vacuum at room temperature**

**Table 3.2  Percent conversion vs. time results for the solid state polymerization of PVCL at open atmosphere**

| Time(hour) | % conversion | Viscosity(dL/g) |
|------------|--------------|-----------------|
| 170        | 35           | 0,2451          |
| 336        | 53           | ......           |
| 460        | 70           | ......           |
| 600        | 83           | .....            |
| 670        | 87           | .....            |
| 890        | 84           | 0,093           |
| 1000       | 94           | 0,093           |
| 1080       | 88           | 0,0845          |
| 1200       | 84           | 0,0745          |
| 1220       | 90           | 0,0778          |
| 1350       | 91           | ......           |
| 1440       | 88           | ......           |
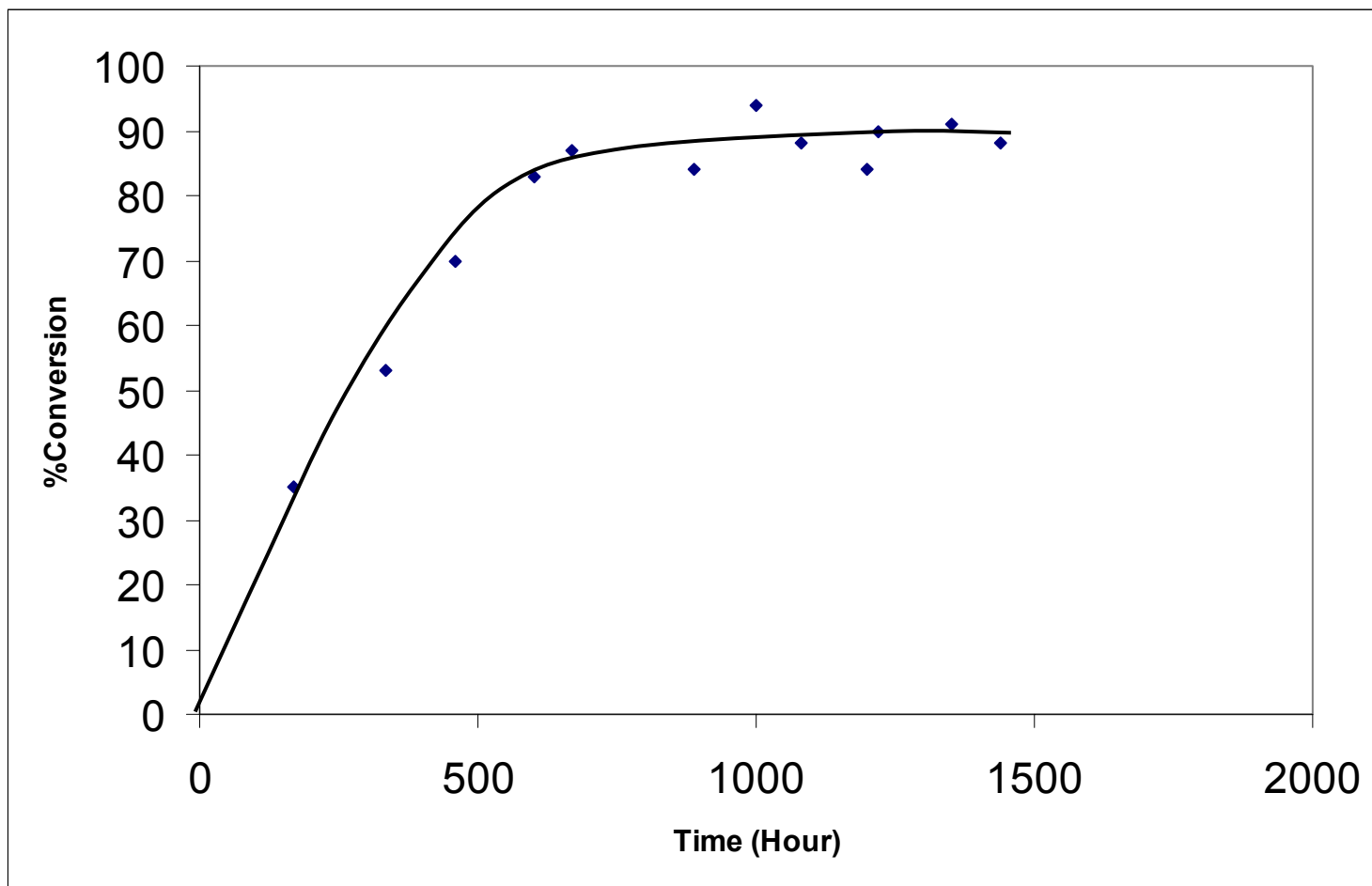
**Figure 3.2  % conversion vs. time graph for solid state polymerization of PVCL at open atmosphere**

## 3.2 MOLECULAR WEIGHT DETERMINATION

The molecular weight determination of polymer was carried out by viscosity, GPC and Light scattering methods. The results for the GPC are tabulated in Table 3.3 .The molecular weight distributions of four samples studied are in the range of 13000-116000. The dispersity index of polymers with molecular weight around 70000 is very close to 1. However the dispersity index for lower molecular weight is very high (about 75) This is related to the conformation of polymer chain. In order to understand it better, the hydrodynamic parameters of the same sample were determined by light scattering methods. The light scattering plotting are given in Figure 3.3 –8. The results are tabulated in Table 3.4. The hydrodynamic radius, $R_h$ and radius of gyration, $R_g$ are expected to increase with molecular weight. In this work there is no systematic change of $R_g$ and $R_h$ with molecular weight. This is due to the different conformational behavior of polymer chains in the solution. The viscosity measurement were also not compatible with obtain molecular weights. The molecular weights of sample by GPC and light scattering are not much different from each other. Therefore, it is mostly conformational differences rather than experimental error in the simple relation of viscosity molecular weight. In this case, the K and α values could not be computed because log(viscosity) versus log(molecular weight) did not give a straight line. The intrinsic viscosity measured are also given in the Table 3.1-2 for the conversion time relation.

**Table 3.3 Results obtained from the GPC measurements**

| Sample | Mw | Mn | Mz | Mp | D | η (measured) |
|--------|--------|--------|-----------|--------|--------|--------------|
| PVCL 1 | 115.700 | 23.480 | 1.522.000 | 39.550 | 4.928 | 0.2568 |
| PVCL 2 | 13.260 | 176 | 102.800 | 2.031 | 75.341 | 0,1821 |
| PVCL 3 | 69.730 | 69.680 | 69.790 | 69.450 | 1.001 | 0,0930 |
| PVCL 4 | 83.830 | 81.430 | 87.220 | 81.870 | 1.029 | 0,0745 |

**Table 3.4 Results obtained from the Light Scattering measurements**

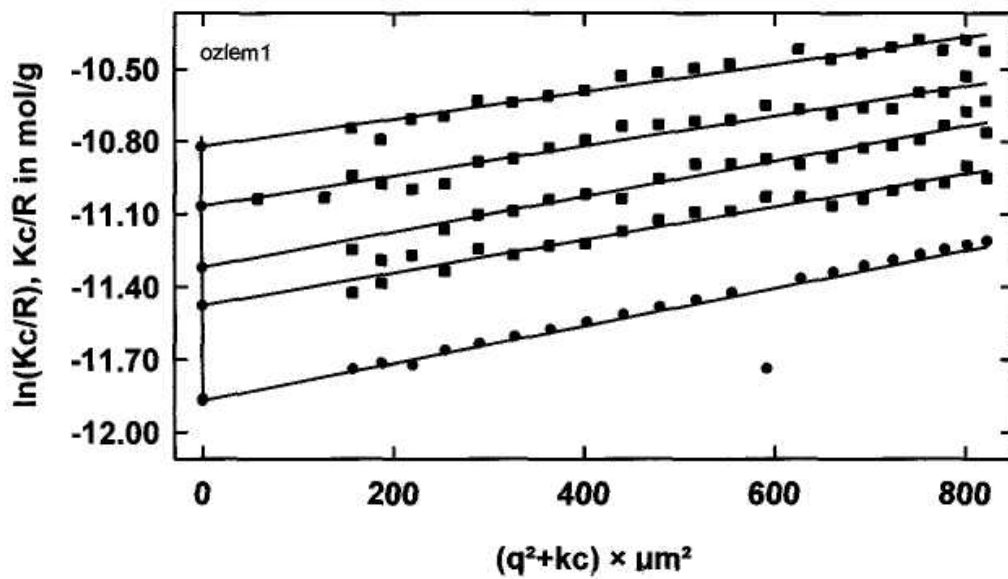| Sample | $M_w$ (g.mole$^{-1}$) | $A_2$ (mole.dm$^3$/g$^2$) | Rg/nm | Rh/nm | Dz | Rg/Rh |
|--------|-----------|---------------|--------|--------|-------|-------|
| PVCL 1 | $1.43\ 10^5$ | $3.99\ 10^{-7}$ | 48.180 | 12.622 | 29.12 | 3.817 |
| PVCL 2 | $1.41\ 10^4$ | $-2.63\ 10^{-5}$ | 72.751 | 29.999 | 12.46 | 2.525 |
| PVCL 3 | $6.93\ 10^4$ | $-2.12\ 10^{-6}$ | 67.943 | 49.717 | 7.56 | 1.367 |
| PVCL 4 | $7.73\ 10^4$ | $-1.39\ 10^{-7}$ | 75.780 | 65.880 | 5.64 | 1.150 |

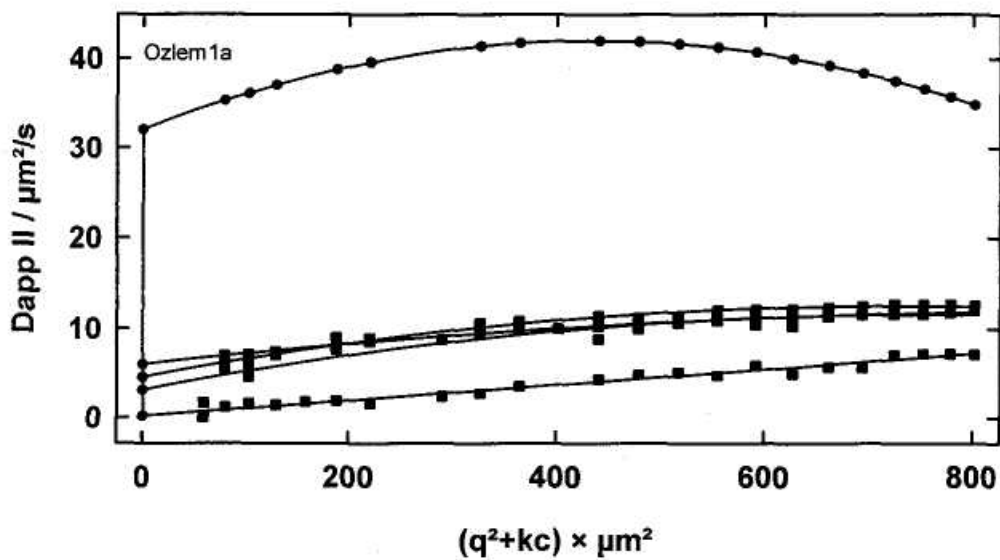**Figure 3.3 Guiner plot of 50% PVCL 1**



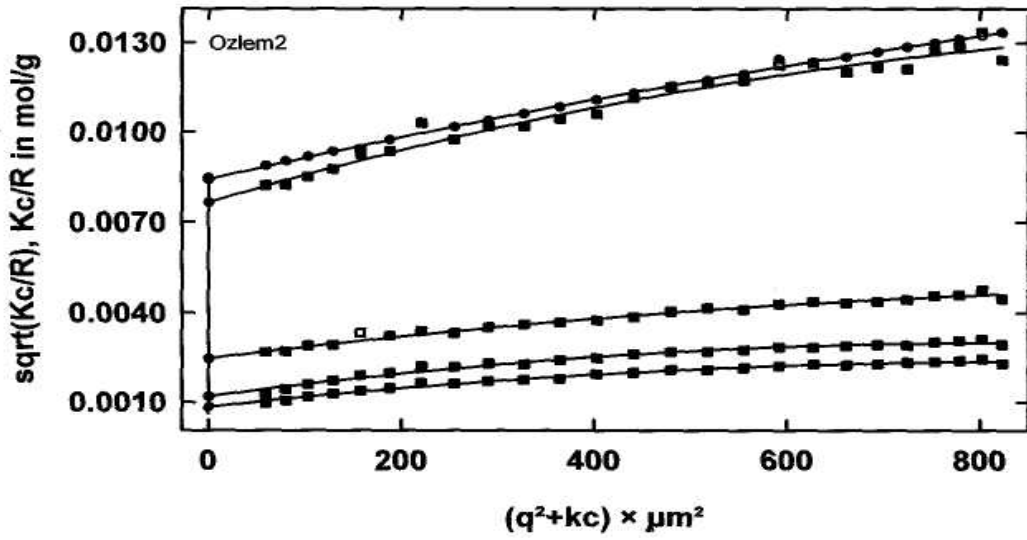**Figure 3.4 Dynamic Light Scattering Results of 50% PVCL 1**

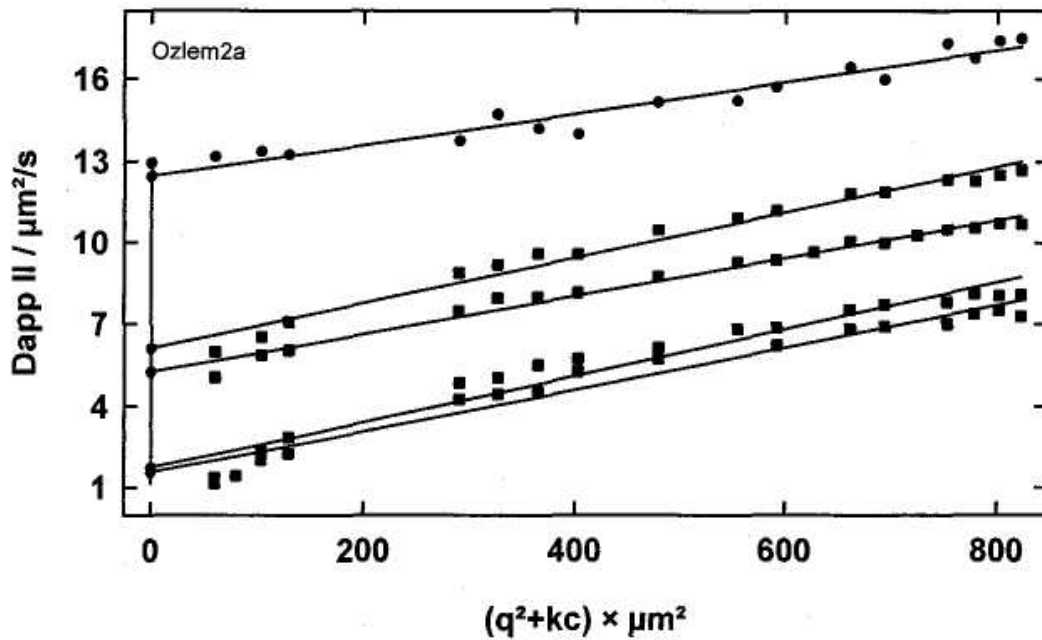**Figure 3.5 Berry plot of 81% PVCL 2**



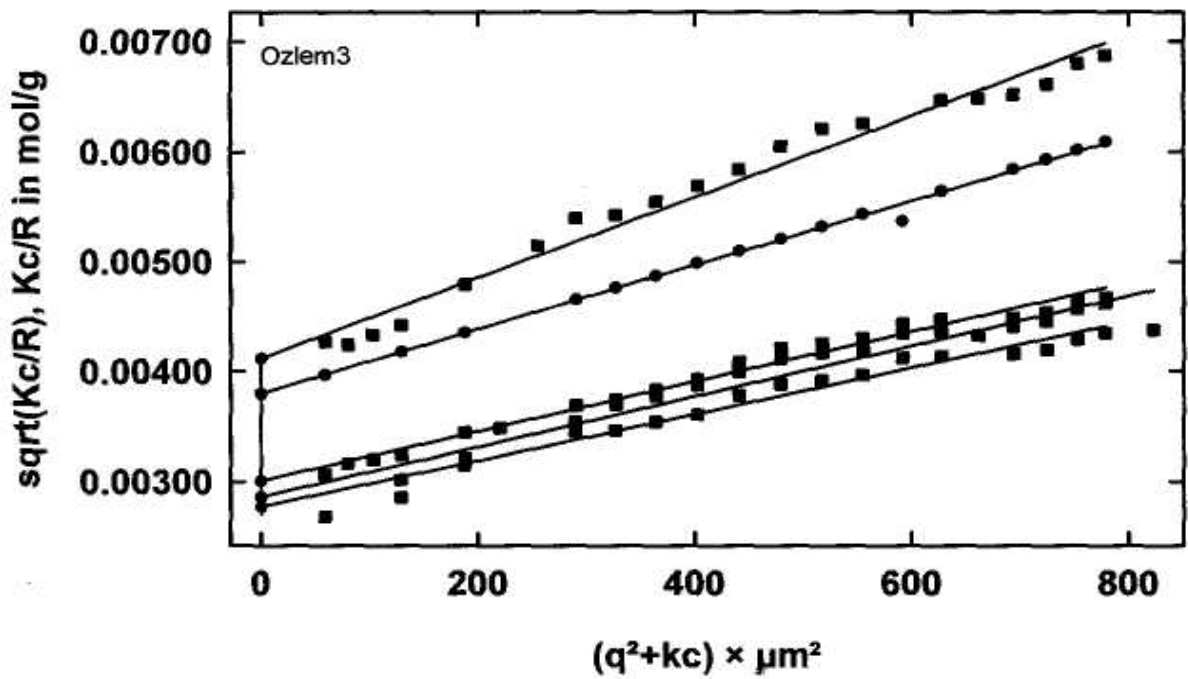**Figure 3.6 Dynamic Light Scattering Results of 81% PVCL 2**
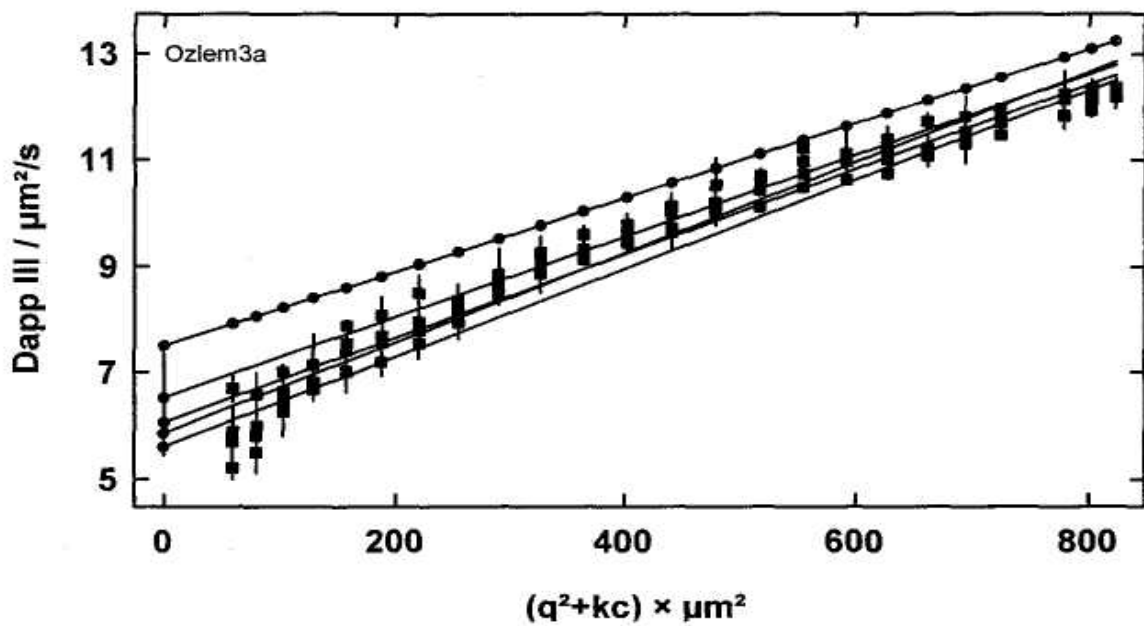
**Figure 3.7 Berry plot of 94% conversion to PVCL 3**



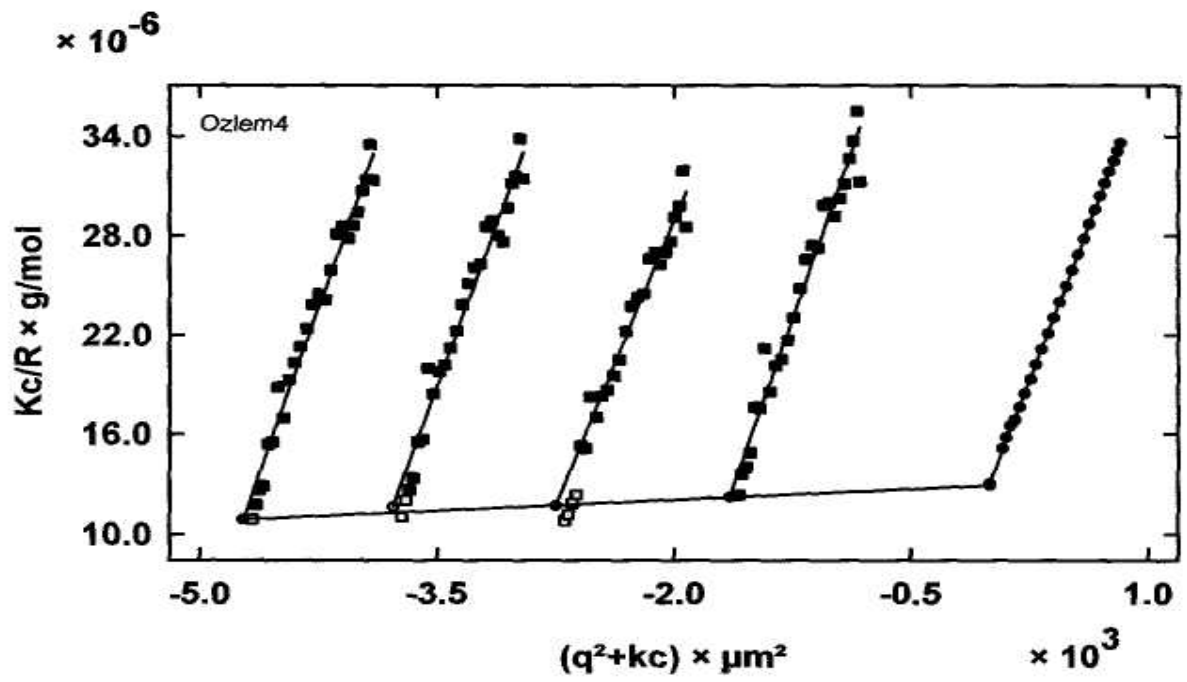**Figure 3.8 Dynamic Light Scattering results of 94% PVCL 3**

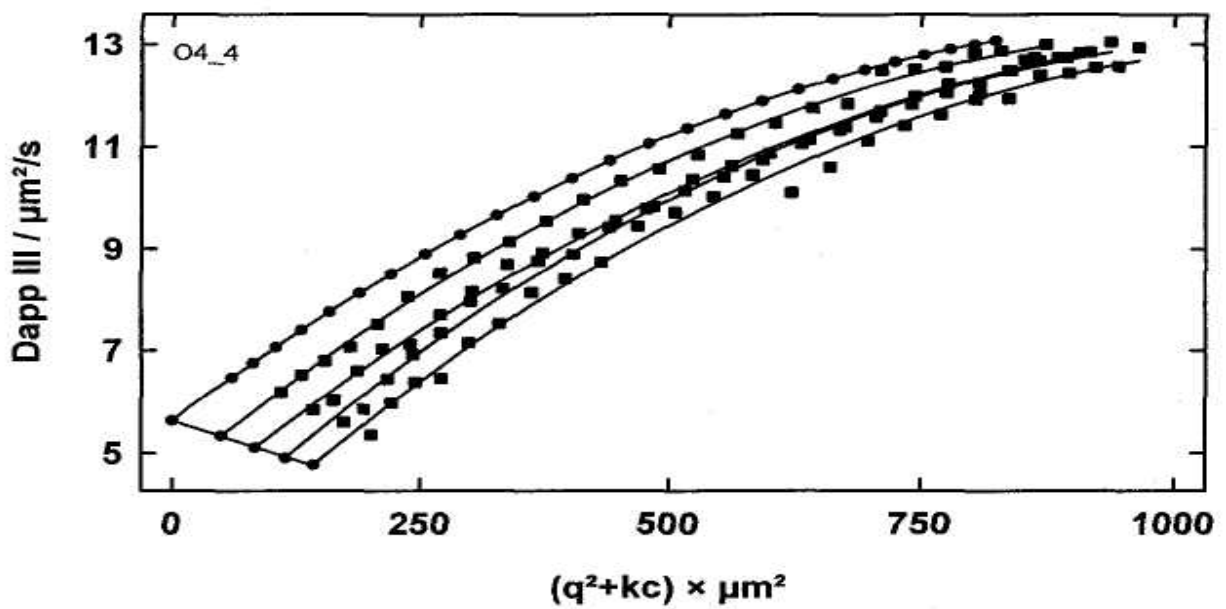**Figure 3.9 Zimm plot of 84% PVCL 4**



**Figure 3.10 Dynamic Light Scattering results of 84% PVCL 4**

## 3.3 FT-IR ANAYSIS

The FT-IR spectra obtained for monomer and polymer are shown in Figures 3.11 and 3-12, respectively. In the IR spectrum of monomer (Figure 3.11), the characteristic carbonyl peak (C=O) is at 1652 cm$^{-1}$. The peaks for the C=C was observed at 1643 cm$^{-1}$ and at 939 cm$^{-1}$. The peaks in the 2921 and 2852 cm$^{-1}$ correspond to the aliphatic C-H stretching. The –CH$_2$- peaks are at 1456-1300 cm$^{-1}$. C-N stretching vibrations are at 1250-1050 cm$^{-1}$. In the spectrum of PVCL (Figure 3.12), C=O bond stretching at 1652 cm$^{-1}$ becomes broader and peak of double bond (-C=C-) near C=O peak disappeared. The aliphatic C-H stretching was observed at 2921 and 2852 cm$^{-1}$. The vinyl, CH$_2$=CH- peak in the spectrum of monomer at 939 cm$^{-1}$ is not observed in the spectrum of polymer. The other vinyl peak at 1643 cm$^{-1}$ is replaced with shifted C=O peak. The CH$_2$ peaks are at about 1456 cm$^{-1}$. Peaks belong to double bond were completely disappeared. The peaks of C-N stretching vibration at 1250-1050 cm$^{-1}$ in the monomer spectrum showed changes in intensity and position in the spectrum of polymer. This might be due to changes in conformation of side group and resonance structures. This can also be observed in the region of 3900-3300 cm$^{-1}$, where new peaks corresponding to the O-H and N-H are observed in the spectrum of polymer. The sharpness of the peaks in polymer spectrum show regularity in polymer molecular chain.

It can be concluded from IR spectra investigation that polymer was successfully achieved and the polymerization proceeds by carbon-carbon double bond opening.
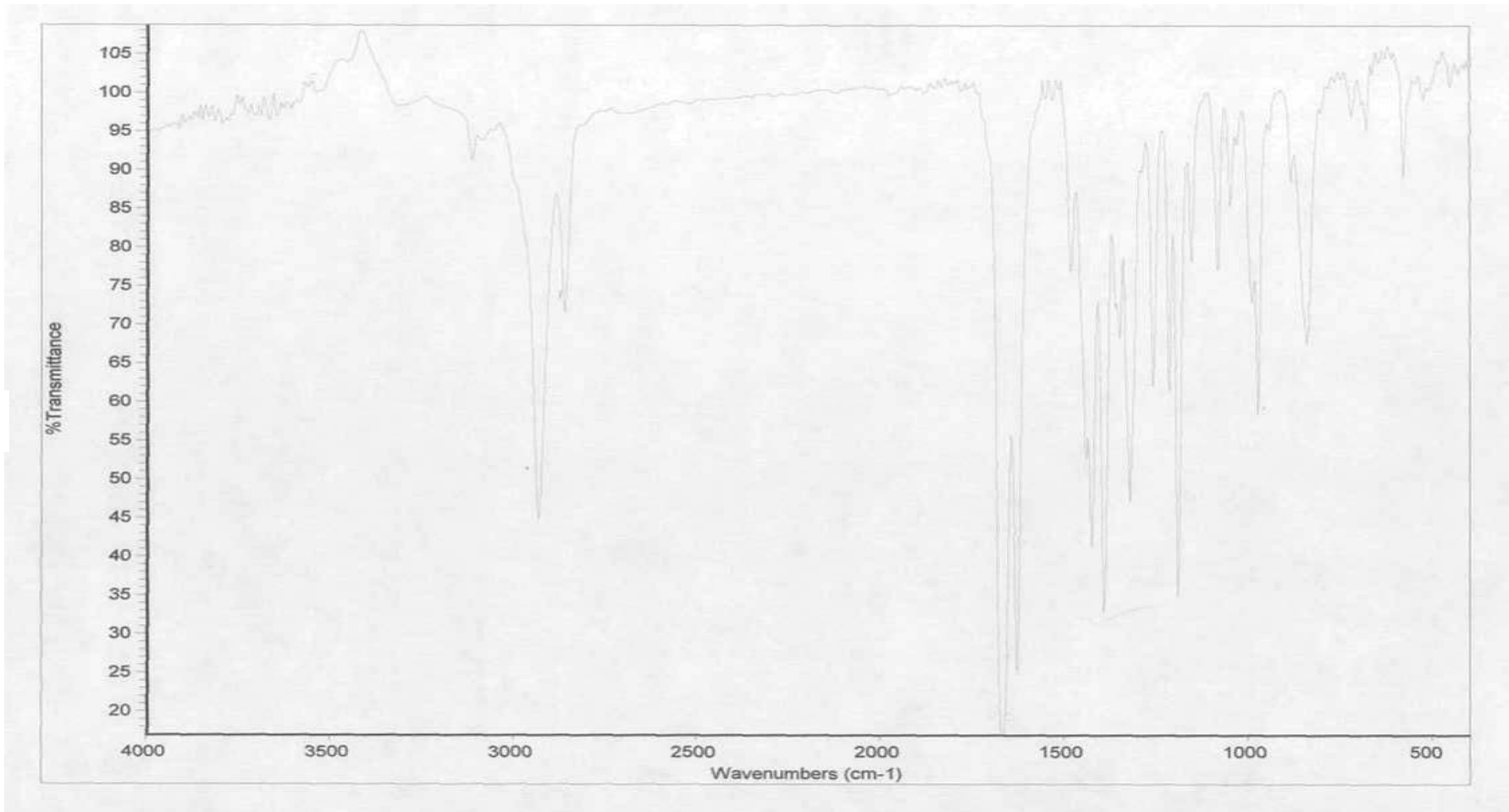
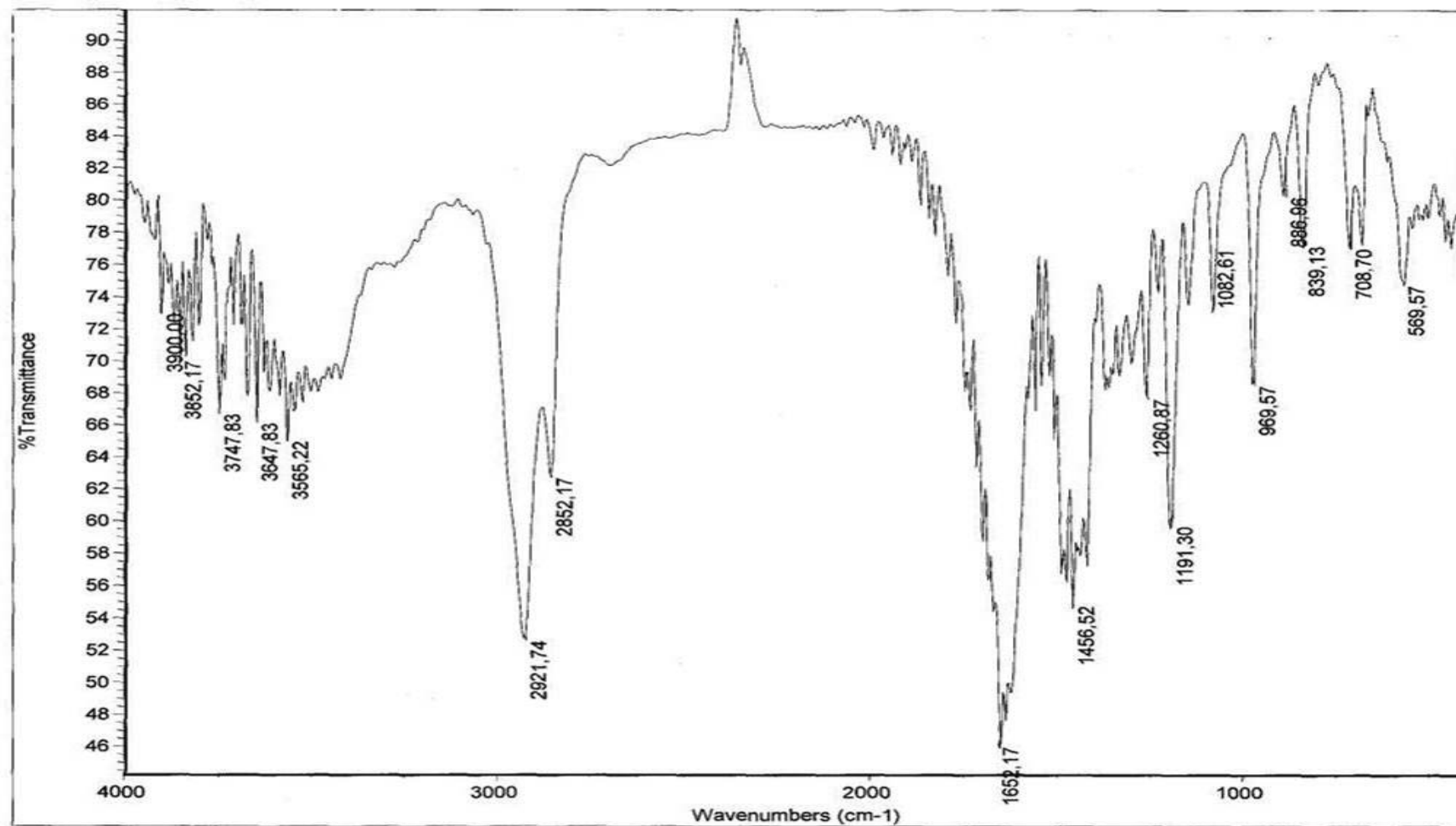**Figure 3.11 FT-IR spectrum of monomer**

**Figure 3.12 FT-IR Spectrum of PVCL**

## 3.4 NUCLEAR MAGNETIC RESONANCE ANALYSIS

The $^{1}$H-NMR and $^{13}$C-NMR spectra of N-vinylcaprolactam monomer and polymer were investigated for the characterization of PVCL. The $^{1}$H-NMR of monomer is shown in Figure 3.13. The peak assignments are shown on the formula of the molecule and in the table as follows. The vinyl group corresponding to b and c are in the 4.33 and 4.45 ppm, respectively. The $CH_2$ groups in the ring as shown with "a" are equivalent and appears at 1.66 ppm. The $CH_2$ groups close to C=O, and N are at 2.53 and 3.4 ppm, respectively. The peaks at 7.26 ppm correspond to solvent (chloroform). These peaks show some changes in the spectrum of polymer as shown Figure 3.14. The vinyl peaks are not completely disappeared upon polymerization but becomes much broader. These peaks correspond to the chain end vinyl groups. This also indicate the presence of oligomers in the polymer samples. When the molecular weight is small, the end group analysis can easily be observed in the NMR spectrum. The other peaks of monomer become much broader in the spectrum of polymer. This is due to the changes in the chair conformation of lactam group in the molecule after changing of intermolecular distance with polymerization.
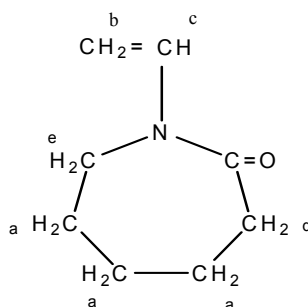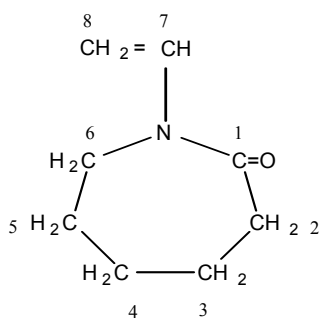


**Table 3.5 The $^{1}$H-NMR spectrum of monomer**

| Proton Type | | Shift (ppm) |
|---|---|---|
| $H_a$ | $CH_2$ | 1.66 |
| $H_b$ | $CH_2$ | 4.33 |
| $H_c$ | =CH-N | 4.45 |
| $H_d$ | $CH_2$ | 2.53 |
| $H_e$ | $CH_2$ | 3.4 |
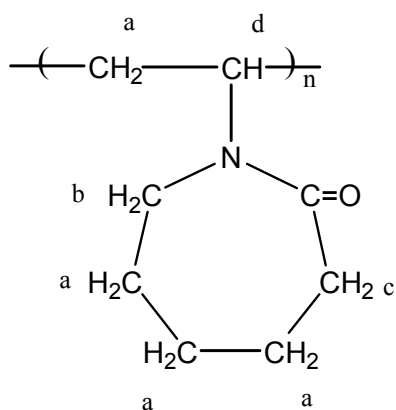
**Table 3.6 The $^1$H-NMR spectrum of polymer**

| Proton Type | Shift (ppm) |
|---|---|
| H$_a$     CH$_2$ | 1.64 |
| H$_b$     CH$_2$ | 2.88 |
| H$_c$   =CH-N | 2.42 |
| H$_d$     CH | 4.16 |

$^{13}$C-NMR spectrum of monomer is given in Figure 3.15. The monomer peaks in the spectrum and the corresponding molecular formula are given as follows: The peak at 77 ppm is due to chloroform. Similar spectrum of polymer is given in Figure 3.16. The CH$_2$= at 93 ppm in the spectrum of monomer is not observed in the spectrum of polymer. However, the methylene peak at 132.4 ppm in the monomer spectrum shifts to 128.3 ppm in the polymer. The CH$_2$ peaks of the monomer are not changing their position in the spectrum of polymer but there intensity becomes much smaller and the peak broadening becomes more. These changes are due to the changes in the conformation of molecules upon polymerization. The preservation of methylene peak at 132.4 ppm (changes to 128.3 ppm) is due to the presence of nitrogen which causes resonance and forming double bond

$$CH_2 = CH$$
8  7

$$H_2C \quad N \quad C=O$$
6  1

$$H_2C \quad \quad CH_2 \quad 2$$
5

$$H_2C \quad CH_2$$
4  3

**Table 3.7 The $^{13}$C-NMR spectrum of monomer**

| C Type | | Shift (ppm) |
|---|---|---|
| $C_1$ | C=O | 174.680 |
| $C_2$ | $CH_2$ | 37.588 |
| $C_3$ | $CH_2$ | 27.602 |
| $C_4$ | $CH_2$ | 23.823 |
| $C_5$ | $CH_2$ | 29.810 |
| $C_6$ | $CH_2$ | 44.427 |
| $C_7$ | $CH_2$ | 132.423 |
| $C_8$ | $CH_2$ | 93.025 |

$$\left( CH_2 - CH \right)_n$$
8  7

$$H_2C \quad N \quad C=O$$
6  1

$$H_2C \quad \quad CH_2 \quad 2$$
5

$$H_2C \quad CH_2$$
4  3
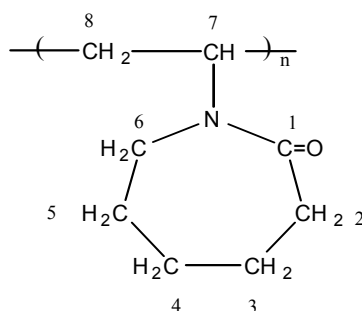
**Table 3.8 The $^{13}$C-NMR spectrum of polymer**

| C (type) | | Shift (ppm) |
|---|---|---|
| $C_1$ | C=O | 176.104 |
| $C_2$ | $CH_2$ | 42.396 |
| $C_3$ | $CH_2$ | 29.911 |
| $C_4$ | $CH_2$ | 23.297 |
| $C_5$ | $CH_2$ | 37.482 |
| $C_6$ | $CH_2$ | 47.260 <br> 46.232 |
| $C_7$ | CH | 128.268 |
| $C_8$ | $CH_2$ | 29.310 |

f polat.001
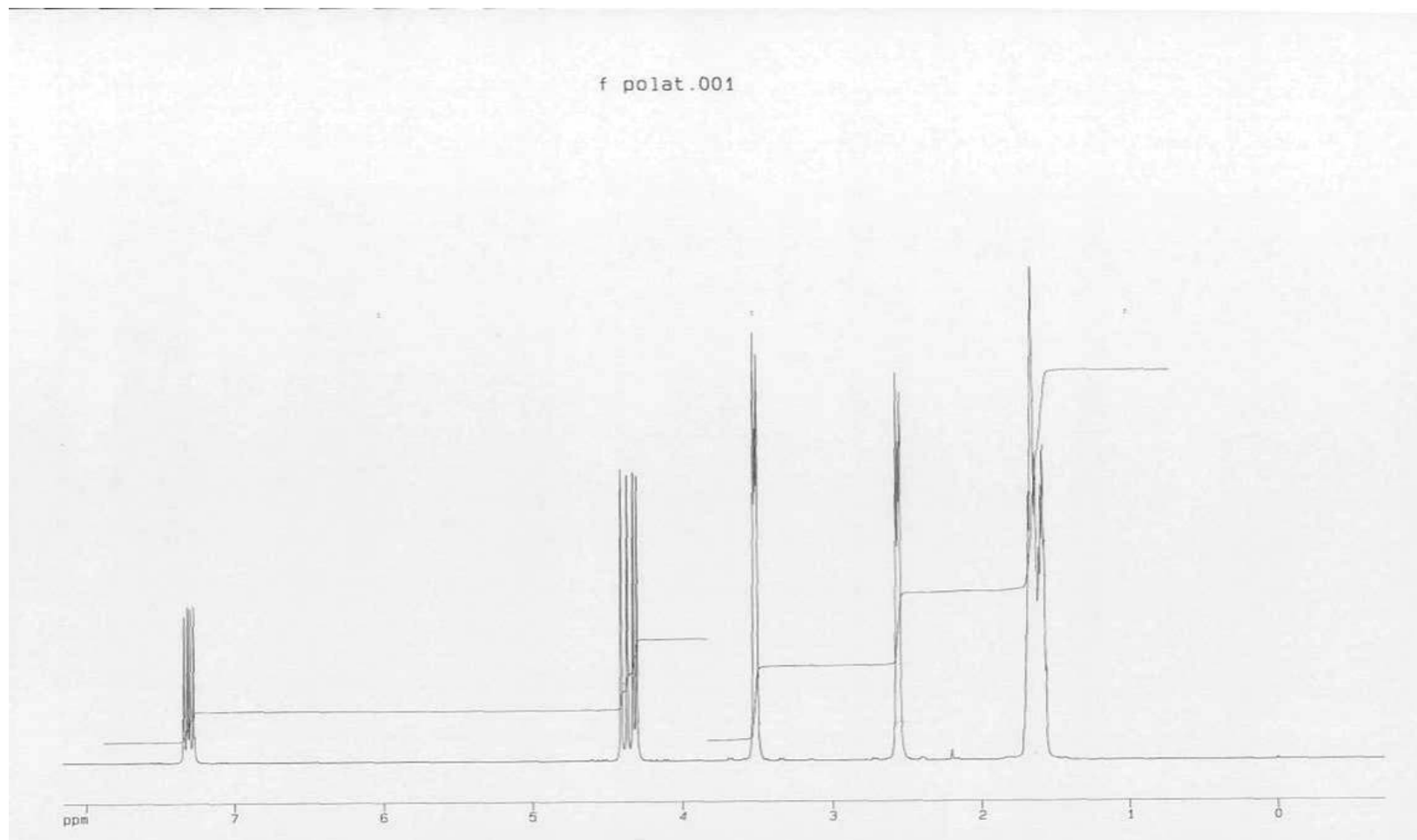


**Figure 3.13 $^1$H-NMR spectrum of monomer**
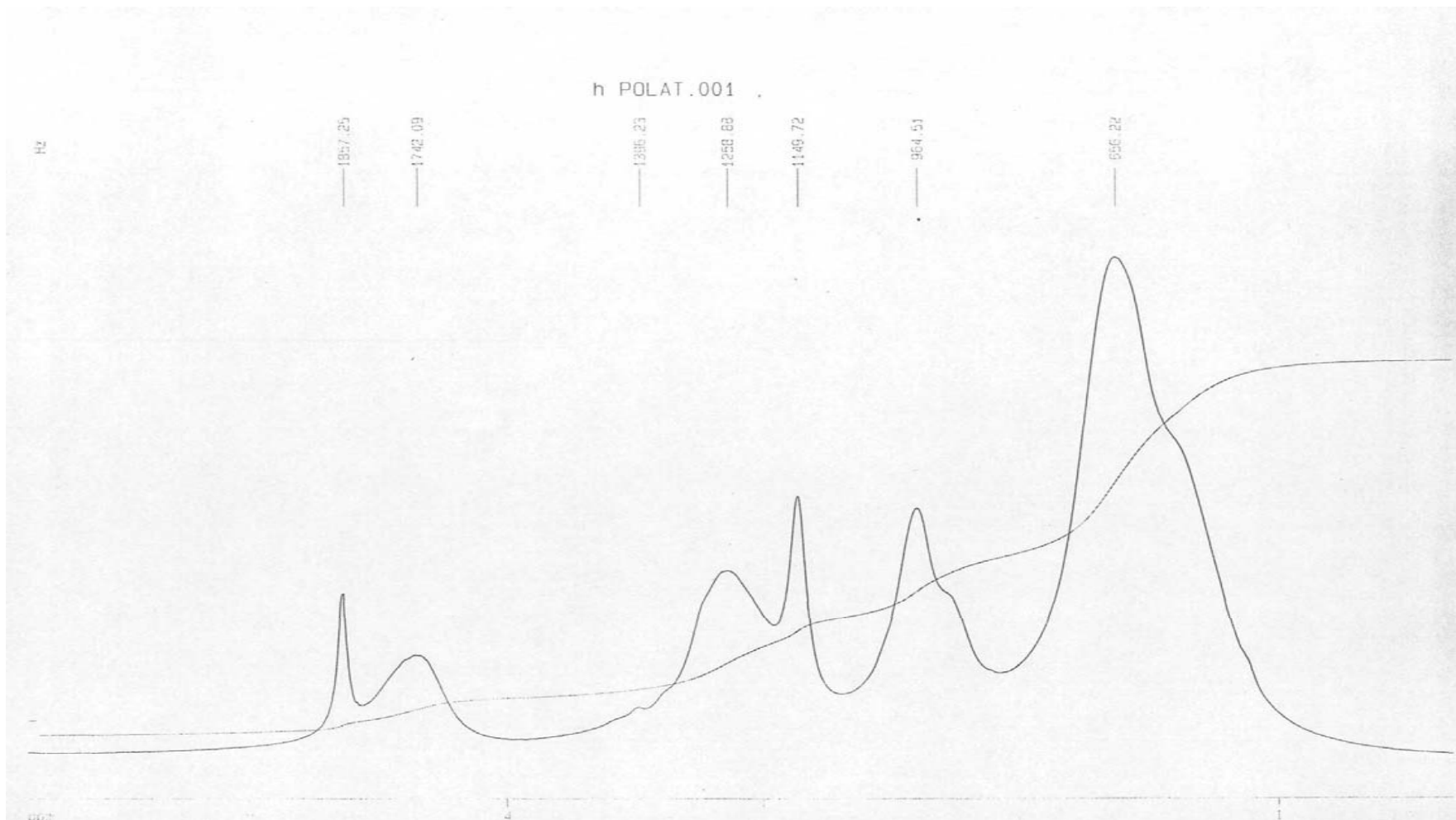
**Figure 3.14 $^1$H-NMR spectrum of polymer**

f polat.002

ppm

174.680

132.423

93.025

77.885
77.566
77.247

44.427

37.588

29.810
27.602
23.823

ppm    200        180        160        140        120        100        80        60        40        20        0

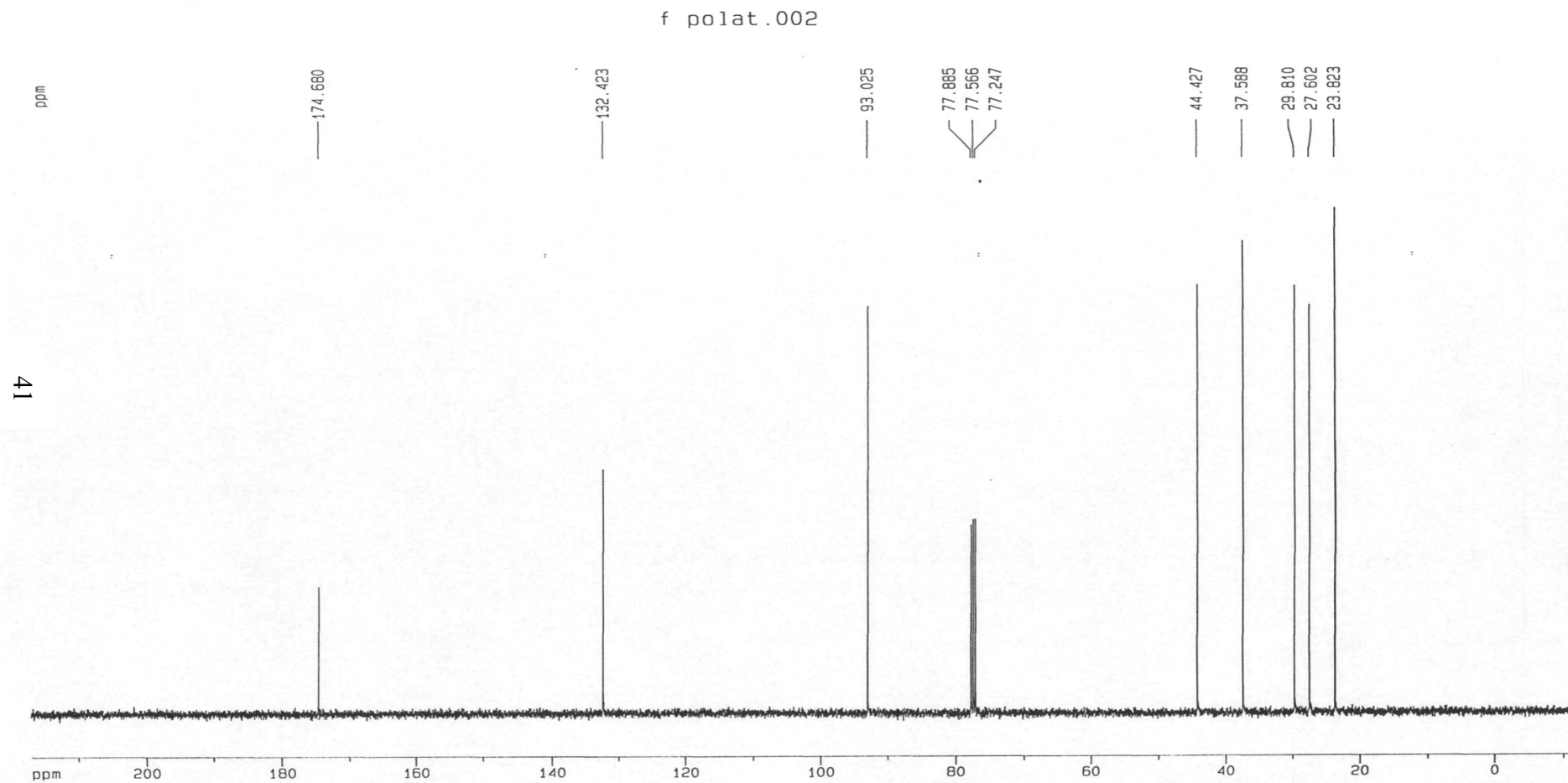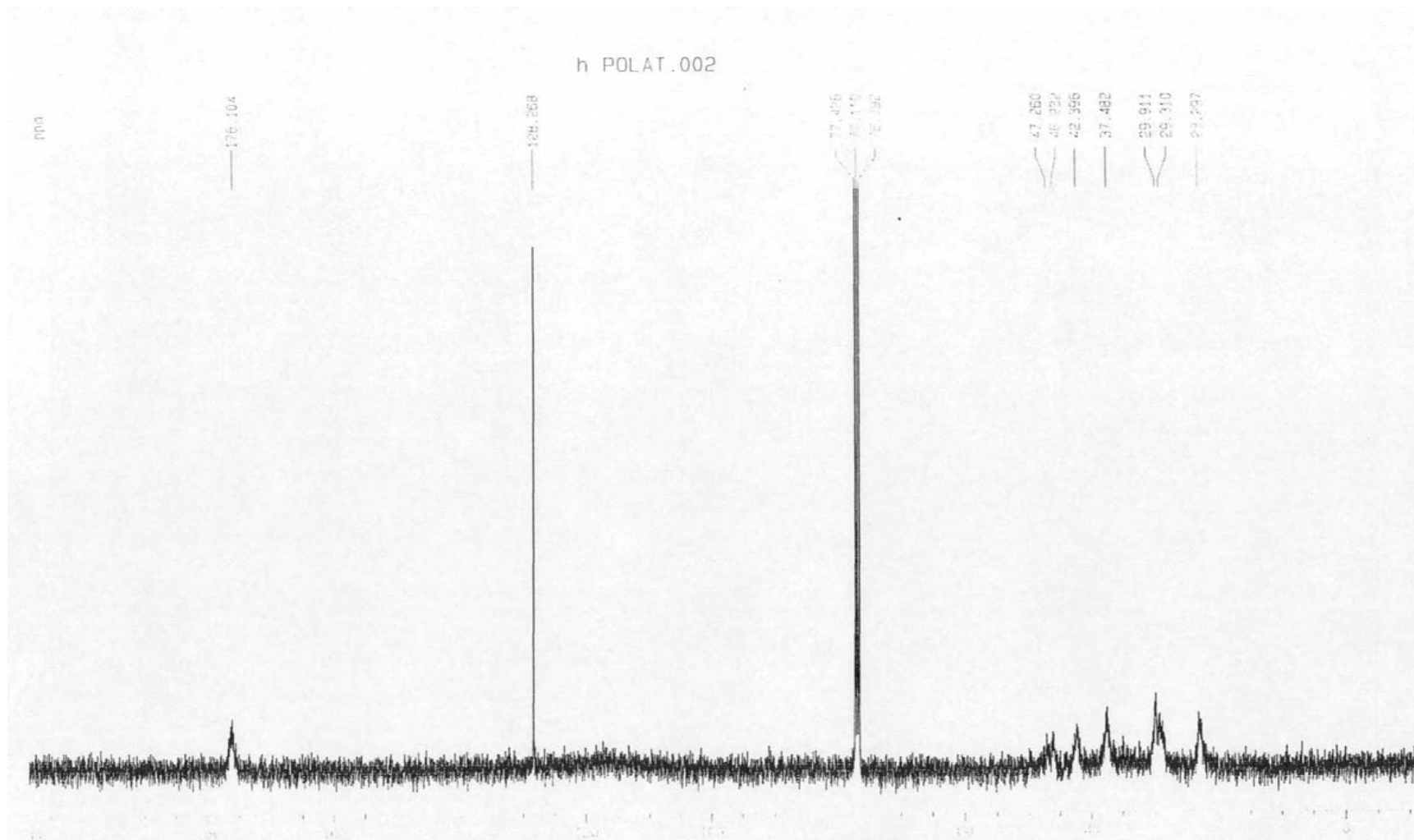**Figure 3.15 $^{13}$C NMR spectrum of monomer**

**Figure 3.16 $^{13}$C NMR spectrum of polymer**

## 3.5 DIFFERENTIAL SCANNING CALORIMETRY

The thermal properties of the monomer and polymers were investigated by DSC method. The DSC thermogram of monomer is given in Figure 3.17. There is an endothermic peak at $34.28^{o}C$ corresponding to the melting point of monomer. The thermogram is recorded in the temperature range of $-50^{o}C$ to $+50^{0}C$ and no other peaks were observed.

The DSC thermogram of the polymers are given in Figure 3.18-23 for different conversion percent to polymer. In the thermogram there is a broad peak at about $100^{o}C$ and less probable peak at about $147^{o}C$ which can be the $T_g$ value. However in order to be sure the sample was cooled and the thermogram of the same sample was taken again. In this thermogram the first peak was disappeared and a new peak of $T_g$ was observed at about $174.6^{o}C$. Therefore the observed peak at about $100^{o}C$ is not $T_g$ but corresponds to further polymerization of small molecular weight fractions or crosslinking. The higher $T_g$ compared to Tg observed before rerun of the thermogram at about $147^{o}C$ is due to the increase of molecular weight.
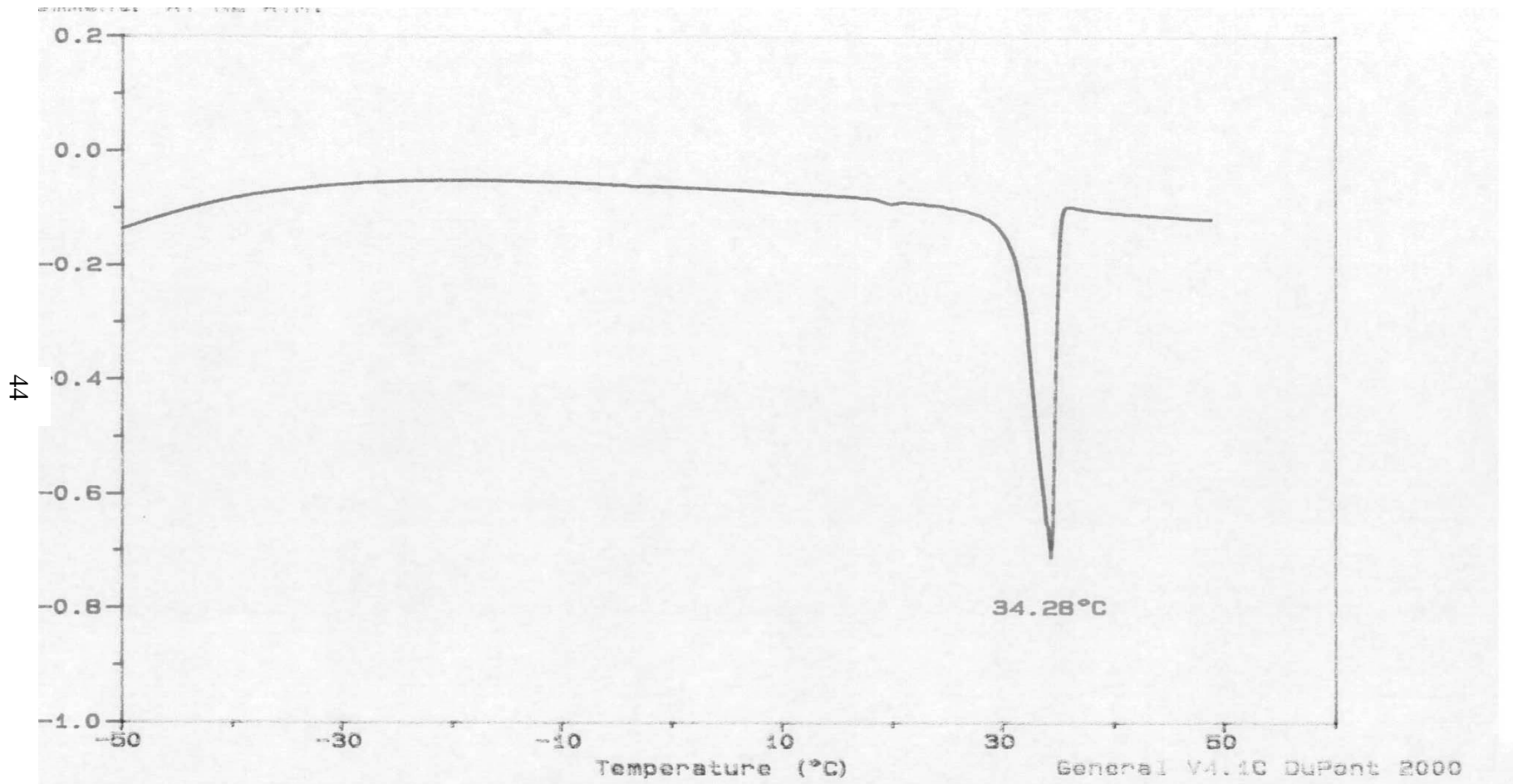
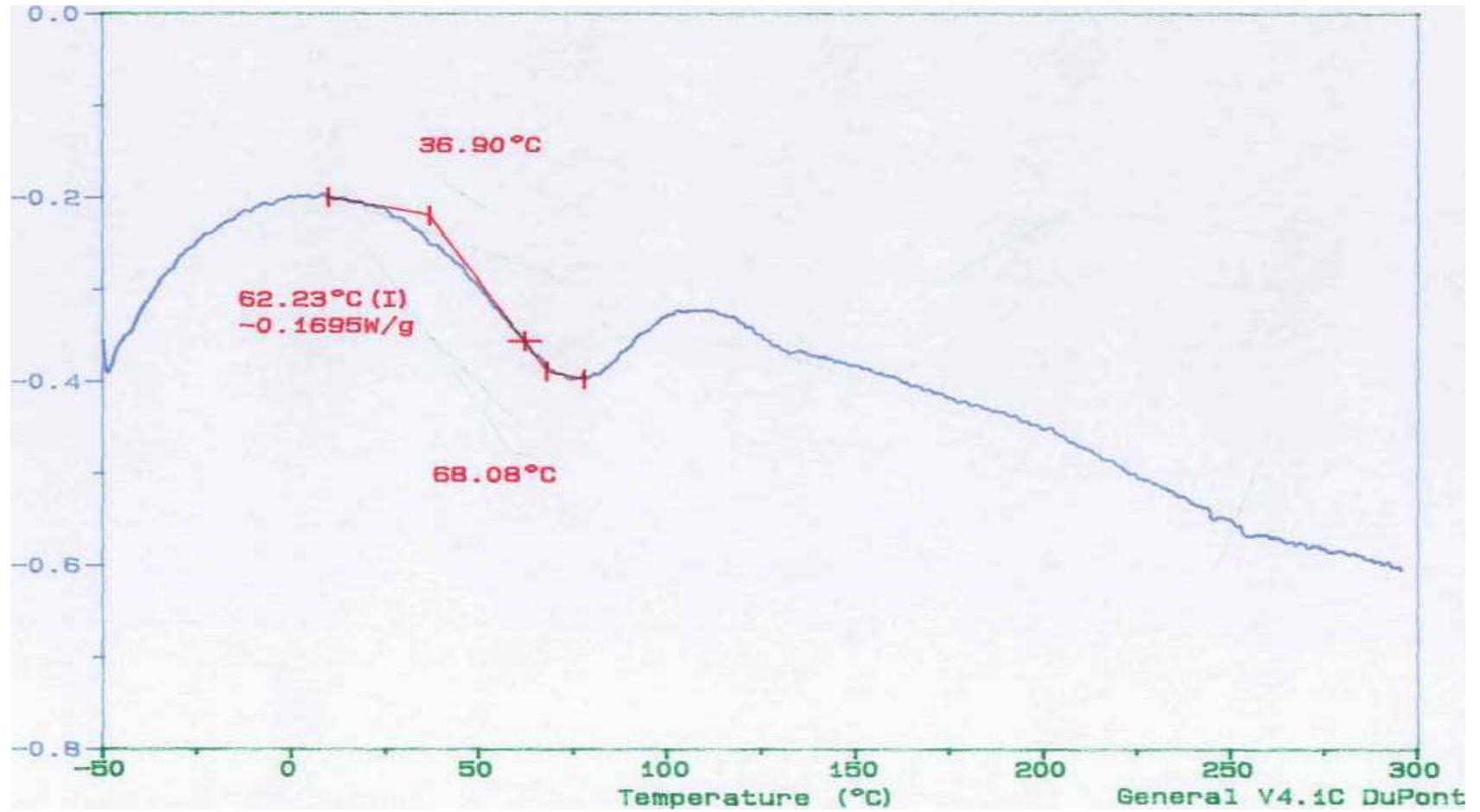**Figure 3.17 DSC diagram of monomer**

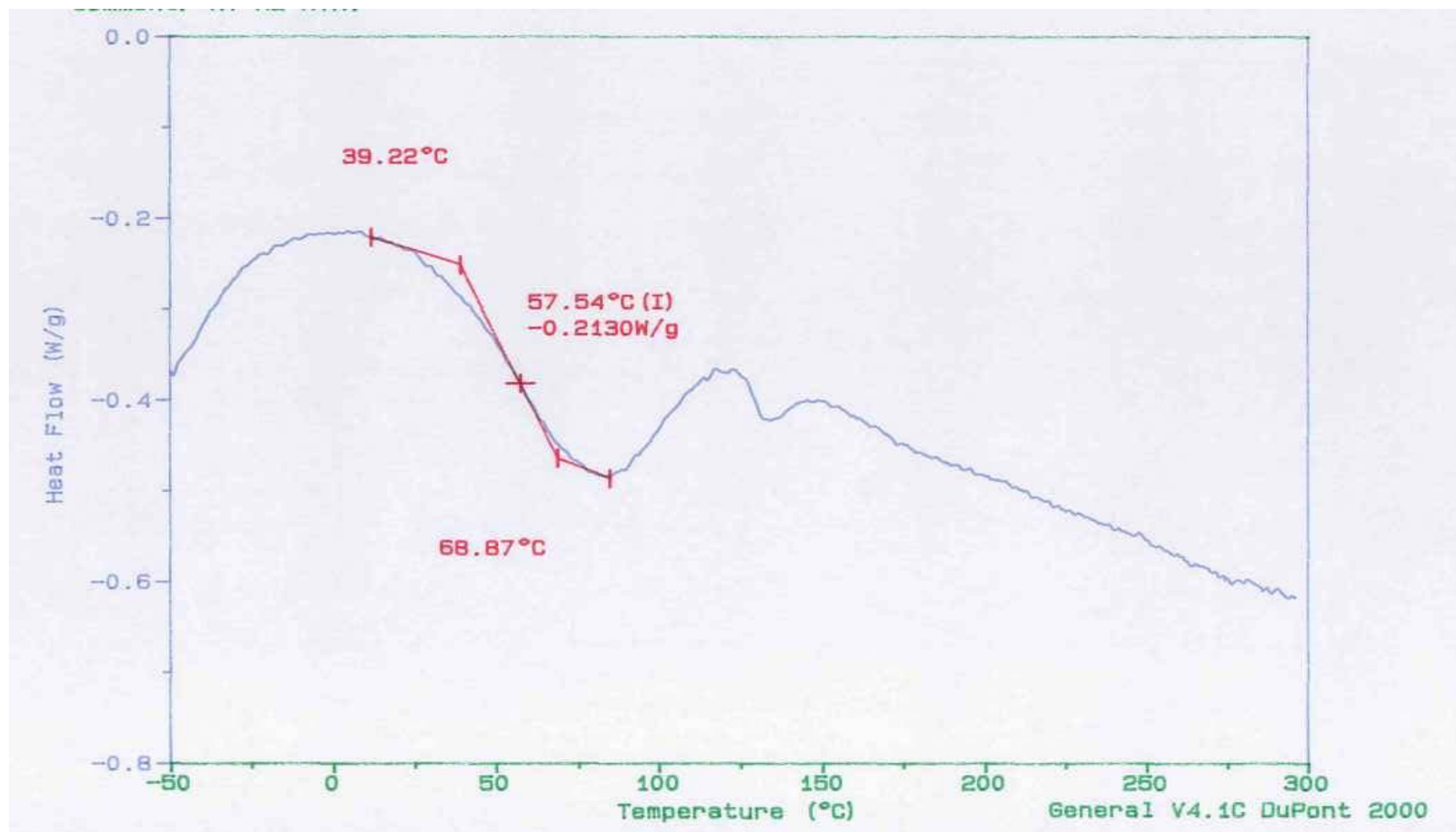**Figure 3.18 DSC diagram of 1% conversion to PVCL**

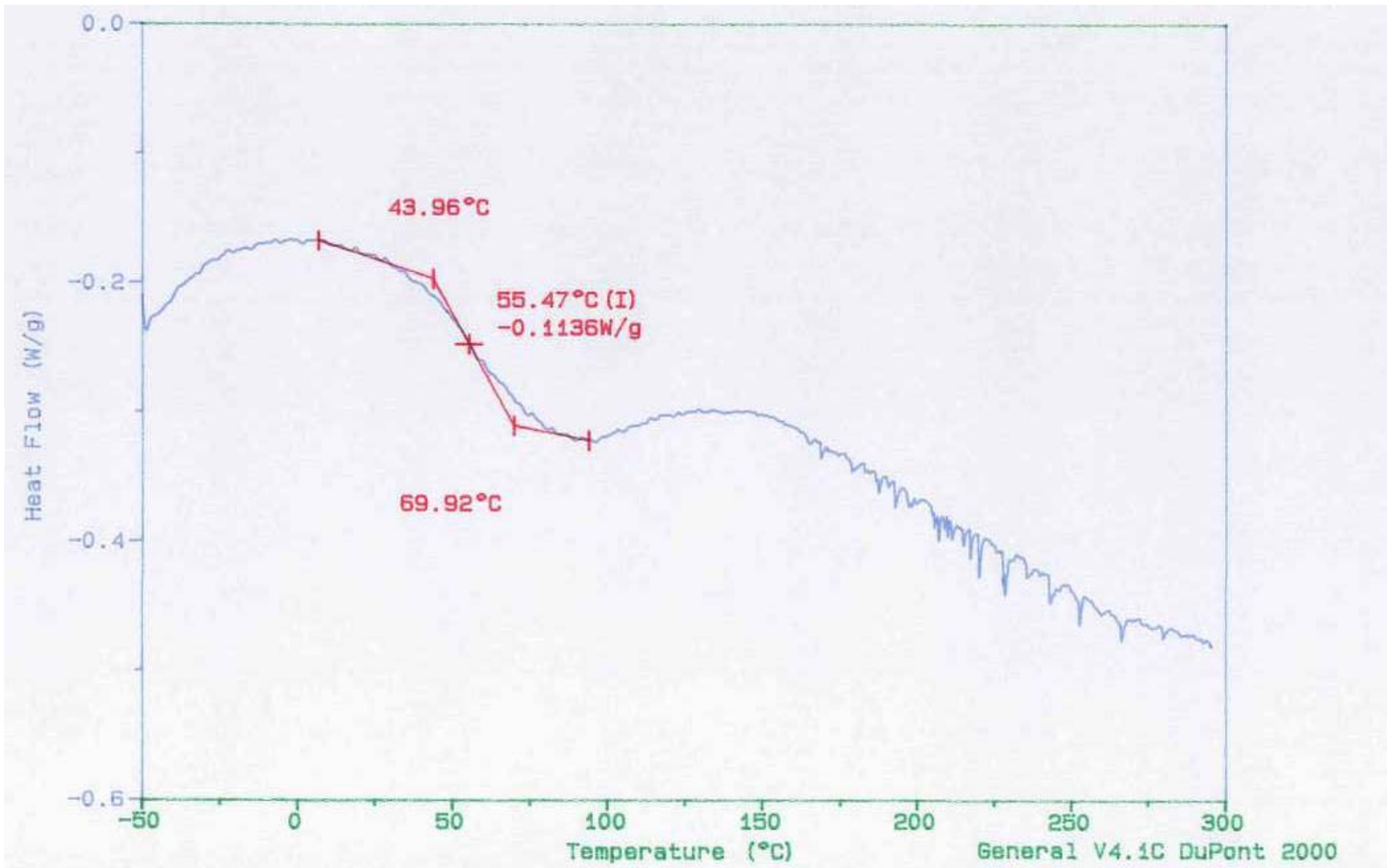**Figure 3.19 DSC diagram of 10% conversion to PVCL**

**Figure 3.20 DSC diagram of 50% conversion to PVCL**
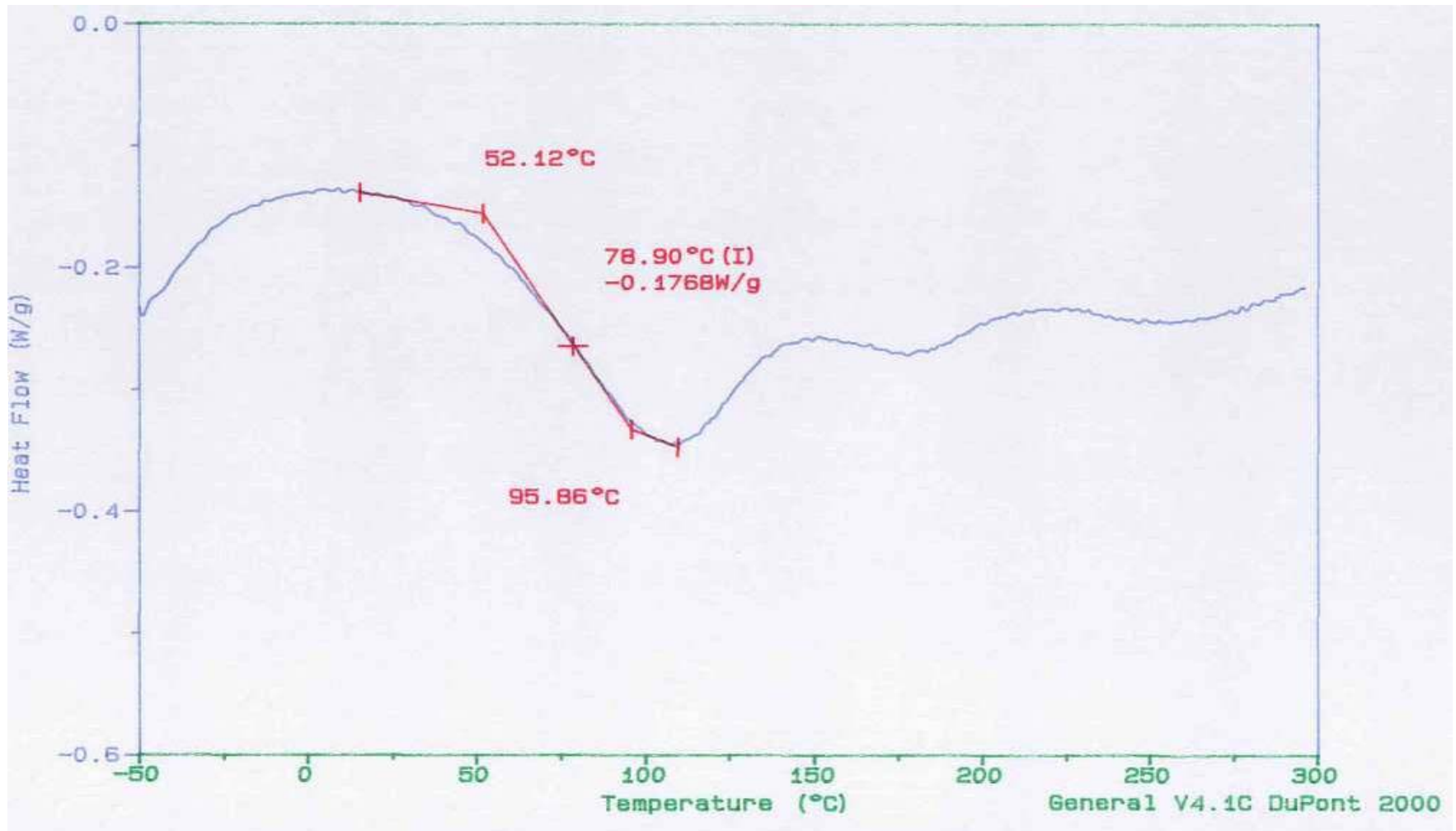
**Figure 3.21 DSC diagram of 94% conversion to PVCL**
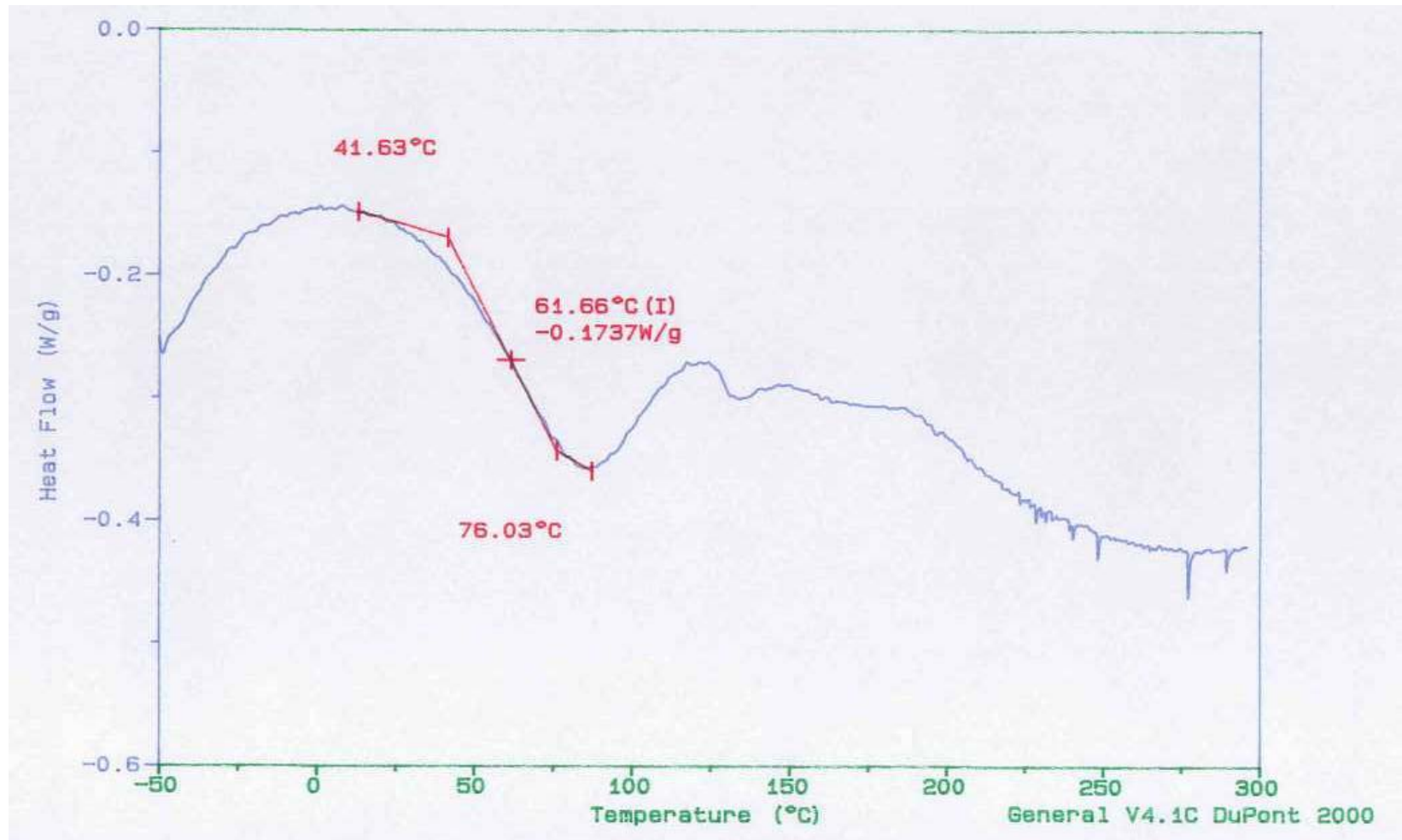
**Figure 3.22 DSC diagram of 96% conversion to PVCL**
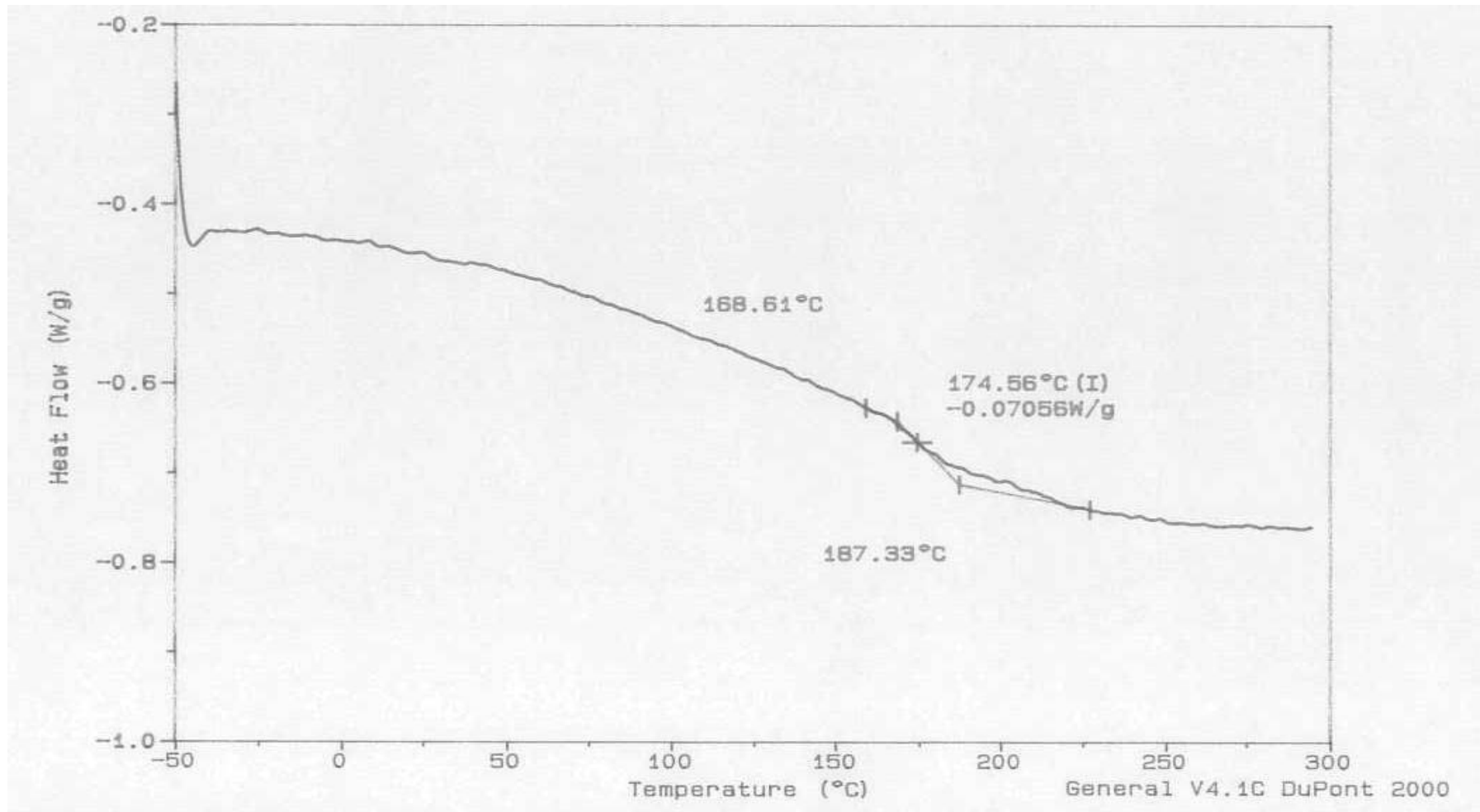
**Figure3.23 DSC  rerun diagram of  96% conversion to PVCL**

50

## 3.6 TGA CHARACTERIZATION OF PVCL

Thermogravimetric analysis of polymer was carried out under nitrogen atmosphere from room temperature up to $900^oC$. The thermogram is given in Figure 3.24. The decreases in weight started at about $70^0C$ and continue up to about $210^0C$ by about 5%. A second range is maximized at $290^0C$. After about $400^0C$ the weight decrease is very sharp and reach to zero percent. The first decomposition corresponds to adsorb water and then crystalline water. The percent weight decrease calculated shows about one mole of water per mole of monomer repeating unit. The main decomposition maximized at $467^0C$. The sharp decrease of weight shows that the degradation of polymer is in the form of depolymerization.
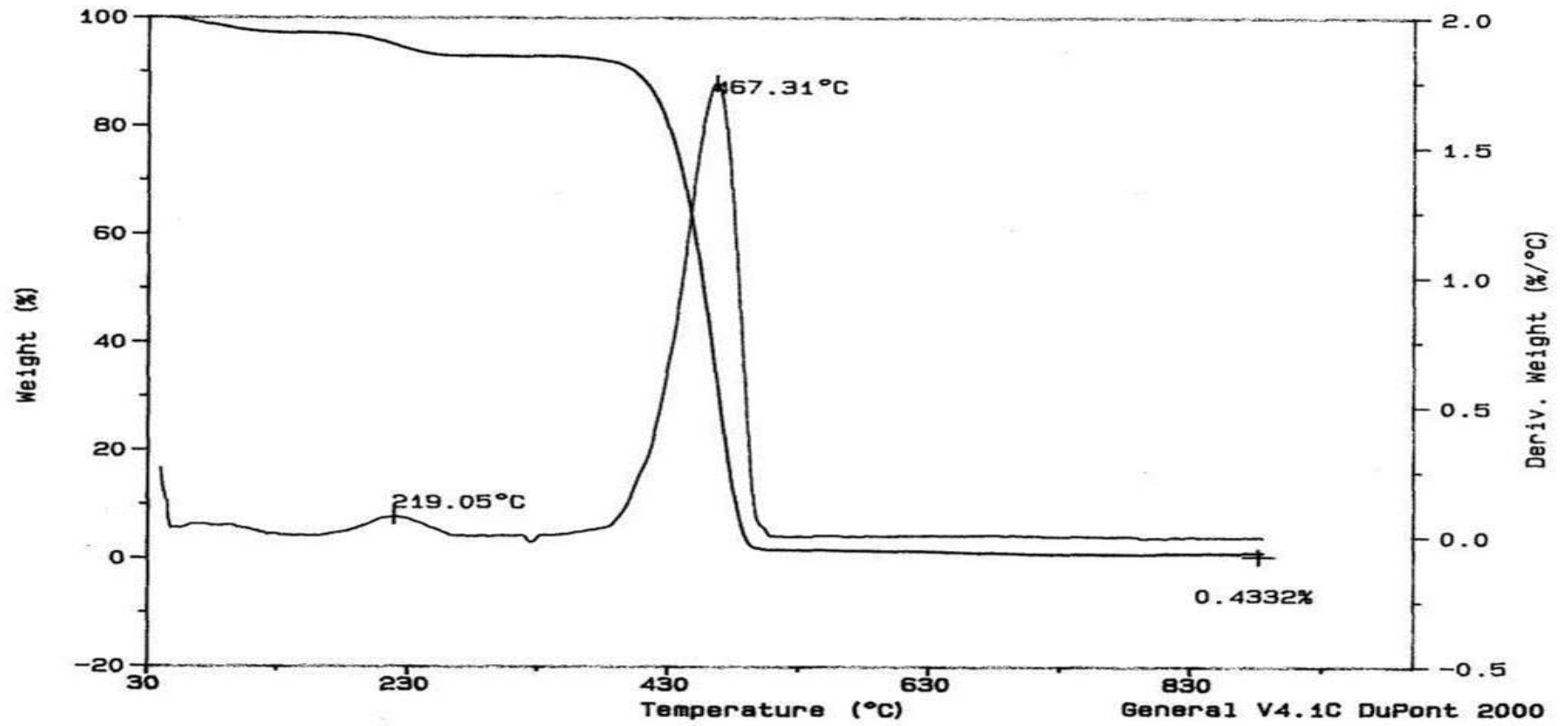
**Figure 3.24 TGA spectrum of PVCL**

## 3.7 X-RAY ANALYSIS

The powder X-Ray spectrum of monomer is given in Figure 3.25.The peaks are very sharp and the intensity is very high. The indexing of peaks were done with cell parameters reported by Tishchenko et al. (25) as a = 8.170(4) A, b = 8.094(4) A, c = 6.799(4) A, $\alpha$ = 99.92(1)$^0$, $\beta$ = 88.89(1)$^0$, $\gamma$ = 115.30(1)$^0$. The most intense peak is due to 010 reflection. The next most intense peak is at 020. Thus, the monomer is aligned in the b-crystallographic axis direction. The intensity and indexing data are tabulated in Table 3.9.

In order to understand the mechanism of polymerization X-ray powder pattern of monomer polymer mixtures after irradiation for several conversions were recorded. This will make a conclusive remark about the change in monomer structure during polymerization. The spectrum of monomer polymer mixtures for 1% conversion to polymer is given in Figure 3.26 and the spectrum data are tabulated in Table 3.10. The intense peak (010) in the spectrum of monomer is retaining its position. However in this case the next intense peak is not at 020. The relative intensity of this peak in the monomer spectrum was 69% but in this spectrum it is only 11%. Instead of the peak at 020, the intensity of $2\bar{1}0$ peak, which was 11% in the spectrum of monomer reach to 36% in this spectra. Other peaks which are weak in the monomer spectrum but become more intense in this spectrum are $0\bar{2}1$ and $\bar{2}11$. Therefore polymerization is most probably proceeds in the direction of 011.

The X-ray powder spectrum of monomer polymer mixture for 10% conversion to polymer is given in Figure 3.27 and the spectrum data are tabulated in Table 3.11. In this spectrum the intensity of peaks are relatively decrease compared to that of monomer in Figure 3.25. However the most intense peak is still 010. The next intense peaks are in similar position as that foe the sample after 1% conversion.

The X-ray powder spectrum of monomer polymer mixture for 50% conversion to polymer is given in Figure 3.28 and the spectrum data are tabulated in Table 3.12. The spectrum shows much differences compared to other spectrum. There is a large decrease in the intensity of monomer peaks and abroad peak corresponding to polymer is appearing in the spectrum. The intensity of $010$ peak is no more the most intense peak (67% intensity). The most intense peak now is $2\bar{2}0$ (100% intensity) .It was only about 12% in the spectrum of monomer. This shows that even at this percent conversion, monomer retain most of its characteristic structure .However, the polymer also shows crystalline structure with appearance of new peaks. Thus, the polymer obtain at 50% conversion has relatively high percent of crystallinity .

The X-ray powder spectrum of monomer polymer mixture for 86% conversion is given in Figure 3.29. The spectrum shows at typical appearance of low percent crystalline polymer. There are some background peaks of monomer also in the spectrum. The structure of monomer is almost completely disappeared in the spectrum. When the polymer is separated from the monomer the X-ray spectrum showed the same pattern. The x-pattern of polymer is given in Figure 3.30.
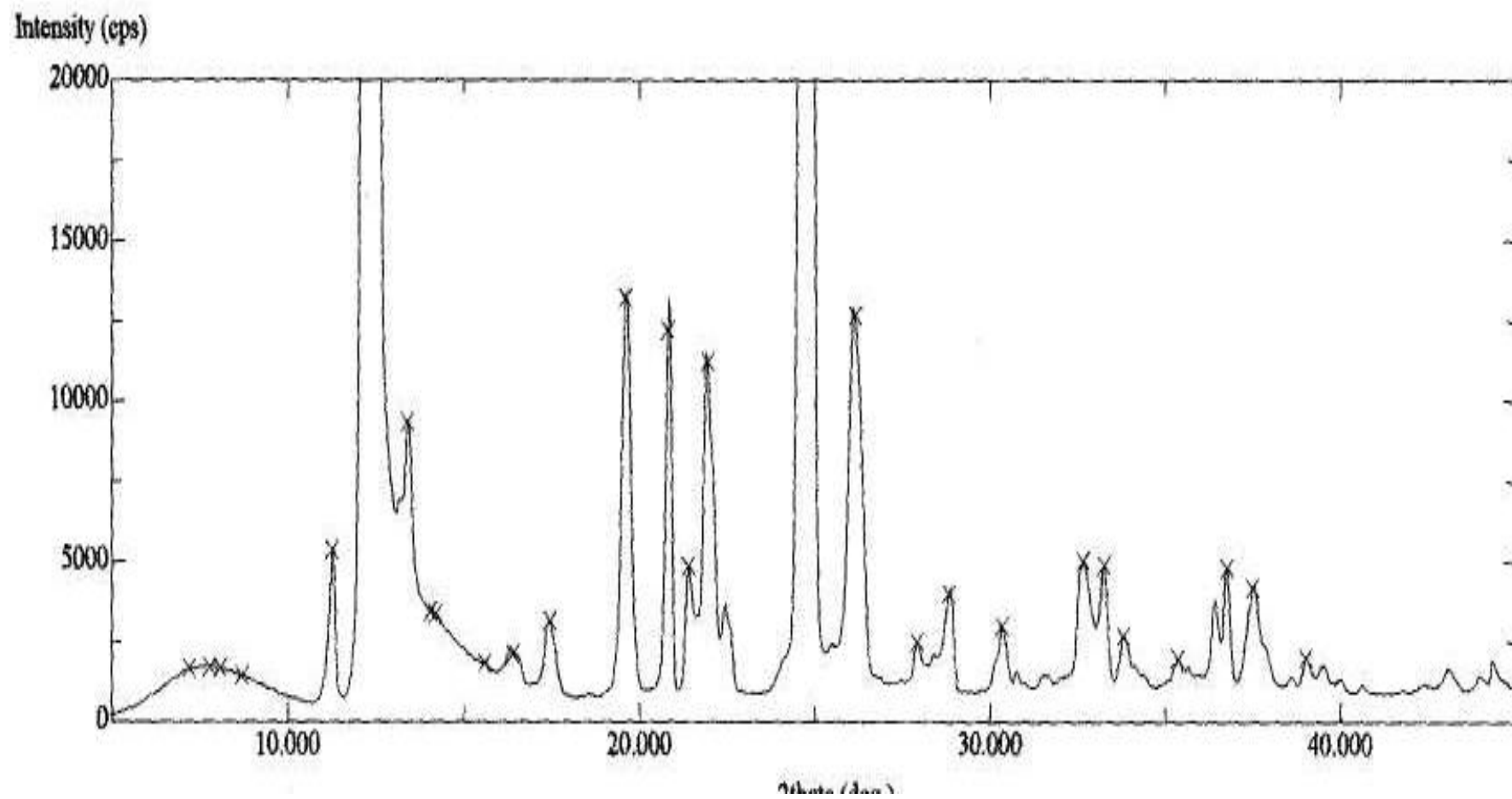
**Figure 3.25 X-Ray spectrum of monomer**

**Table 3.9 X-Ray Analysis of Monomer**

| Peak no | 2θ | d-Value | Intensity | I/Io | d-calc. | h | k | l |
|---------|------|--------|-----------|------|---------|-----|-----|-----|
| 1 | 11,25 | 7,8584 | 5370 | 5 | | | | |
| 2 | 12,40 | 7,132 | 111176 | 100 | 7,1962 | 0 | 1 | 0 |
| 3 | 13,40 | 6,602 | 9369 | 9 | 6,6849 | 0 | 0 | 1 |
| 4 | 17,45 | 5,0778 | 3156 | 3 | 5,0777 | 1 | -1 | 1 |
| 5 | 19,60 | 4,5253 | 13230 | 12 | 4,5209 | -1 | 1 | 1 |
| 6 | 20,85 | 4,2568 | 13207 | 12 | 4,3058 | 1 | 1 | 0 |
| 7 | 21,95 | 4,0459 | 11230 | 11 | 4,0676 | 2 | -1 | 0 |
| 8 | 22,45 | 3,9569 | 3682 | 4 | 3,9784 | 1 | -2 | 0 |
| 9 | 24,8 | 3,587 | 76173 | 69 | 3,5981 | 0 | 2 | 0 |
| 10 | 26.15 | 3,4048 | 12678 | 12 | 3,4034 | 1 | 1 | 1 |
| 11 | 27,90 | 3,1951 | 2480 | 3 | 3,192 | 2 | -2 | 1 |
| 12 | 28,8 | 3,0973 | 4004 | 4 | 3,1165 | -1 | 0 | 2 |
| 13 | 30,35 | 2,9425 | 2974 | 3 | 2,9526 | 0 | 2 | 1 |
| 14 | 30,75 | 2,9051 | 1598 | 2 | 2,9058 | -2 | 2 | 1 |
| 15 | 32,65 | 2,7403 | 5032 | 5 | 2,7429 | -1 | -2 | 1 |
| 16 | 33,25 | 2,6922 | 4881 | 5 | 2,7059 | 0 | -2 | 2 |
| 17 | 33,8 | 2,6496 | 2684 | 3 | 2,6398 | 1 | -3 | 0 |
| 18 | 35,35 | 2,5369 | 1987 | 2 | 2,5388 | -2 | 1 | 2 |
| 19 | 36,4 | 2,4661 | 3803 | 4 | 2,4575 | 3 | 0 | 0 |
| 20 | 36,75 | 2,4434 | 4824 | 5 | 2,4395 | 1 | 2 | 1 |
| 21 | 37,5 | 2,3963 | 4205 | 4 | 2,3987 | 0 | 3 | 0 |
| 22 | 39 | 2,3075 | 2017 | 2 | 2,3185 | -1 | 3 | 1 |

**Figure 3.26 X-Ray spectrum of monomer-polymer (1% PVCL) mixture**

**Table 3.10 X-Ray Analysis of monomer-polymer ( 1% PVCL) mixture**

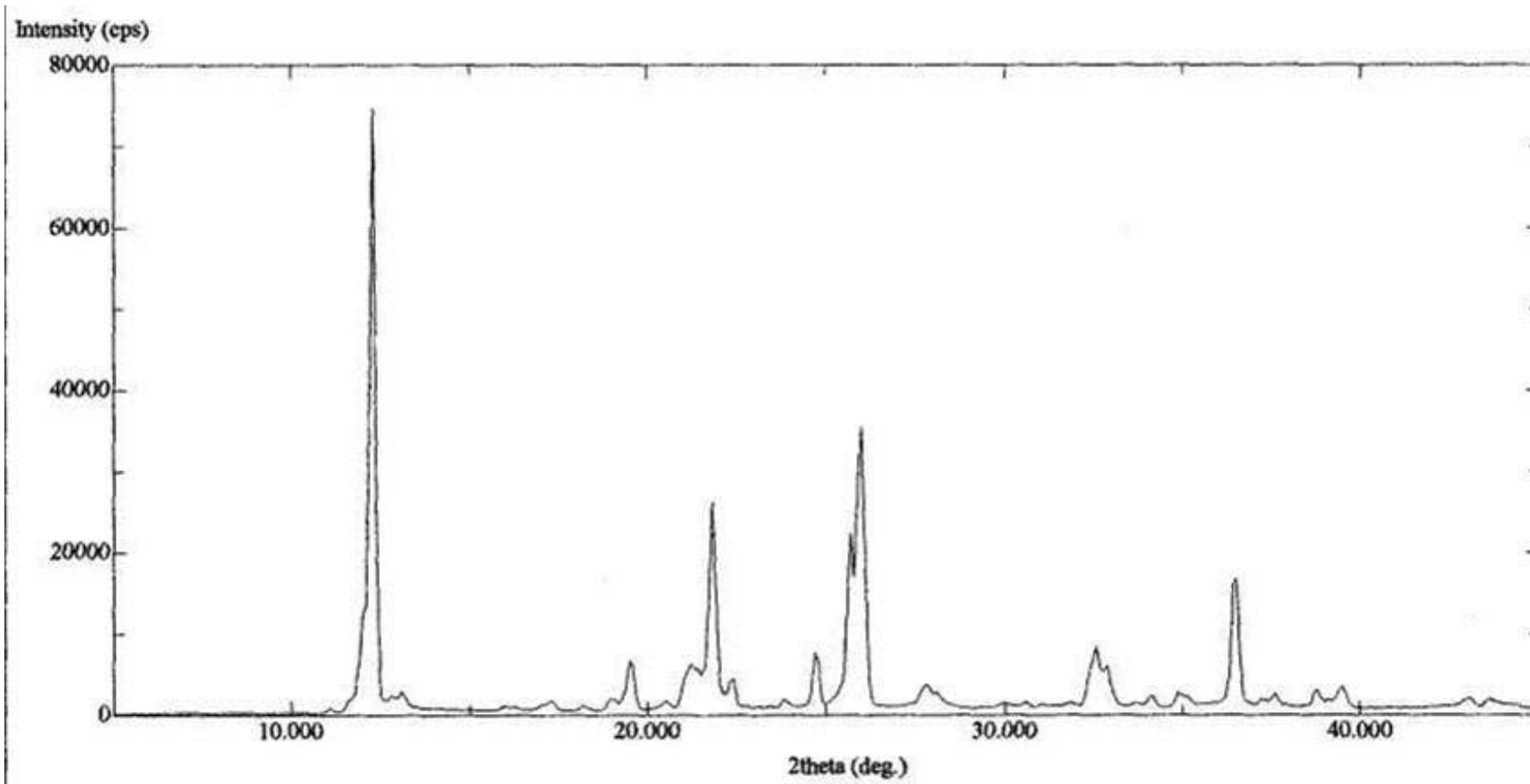| peak no | 2θ | d-Value | Intensity | I/Io | d-calc. | h | k | l |
|---------|------|---------|-----------|------|---------|----|----|----|
| 1 | 12 | 7,3689 | 11523 | 16 | 7,3726 | 1 | 0 | 0 |
| 2 | 12,3 | 7,1898 | 74741 | 100 | 7,1962 | 0 | 1 | 0 |
| 3 | 19,5 | 4,5483 | 6656 | 9 | 4,5209 | -1 | 1 | 1 |
| 4 | 21,8 | 4,0734 | 26181 | 36 | 4,0676 | 2 | -1 | 0 |
| 5 | 22,4 | 3,9656 | 4428 | 6 | 3,9784 | 1 | -2 | 0 |
| 6 | 24,7 | 3,6013 | 7795 | 11 | 3,5981 | 0 | 2 | 0 |
| 7 | 25,7 | 3,4634 | 22294 | 30 | 3,4394 | 0 | -2 | 1 |
| 8 | 26.0 | 3,4241 | 35416 | 48 | 3,4216 | -2 | 1 | 1 |
| 9 | 27,8 | 3,2063 | 3807 | 6 | 3,192 | 2 | -2 | 1 |
| 10 | 32,6 | 2,7444 | 8448 | 12 | 2,7429 | -1 | -2 | 1 |
| 11 | 34,1 | 2,627 | 2414 | 4 | 2,6284 | 2 | -1 | 2 |
| 12 | 34,9 | 2,5686 | 2914 | 4 | 2,582 | 2 | -3 | 0 |
| 13 | 36,5 | 2,4596 | 16785 | 23 | 2,4575 | 3 | 0 | 0 |
| 14 | 37,6 | 2,3901 | 2670 | 4 | 2,3987 | 0 | 3 | 0 |
| 15 | 38,8 | 2,3189 | 3119 | 5 | 2,3185 | -1 | 3 | 1 |
| 16 | 39,5 | 2,2794 | 3535 | 5 | 2,278 | 1 | -3 | 2 |

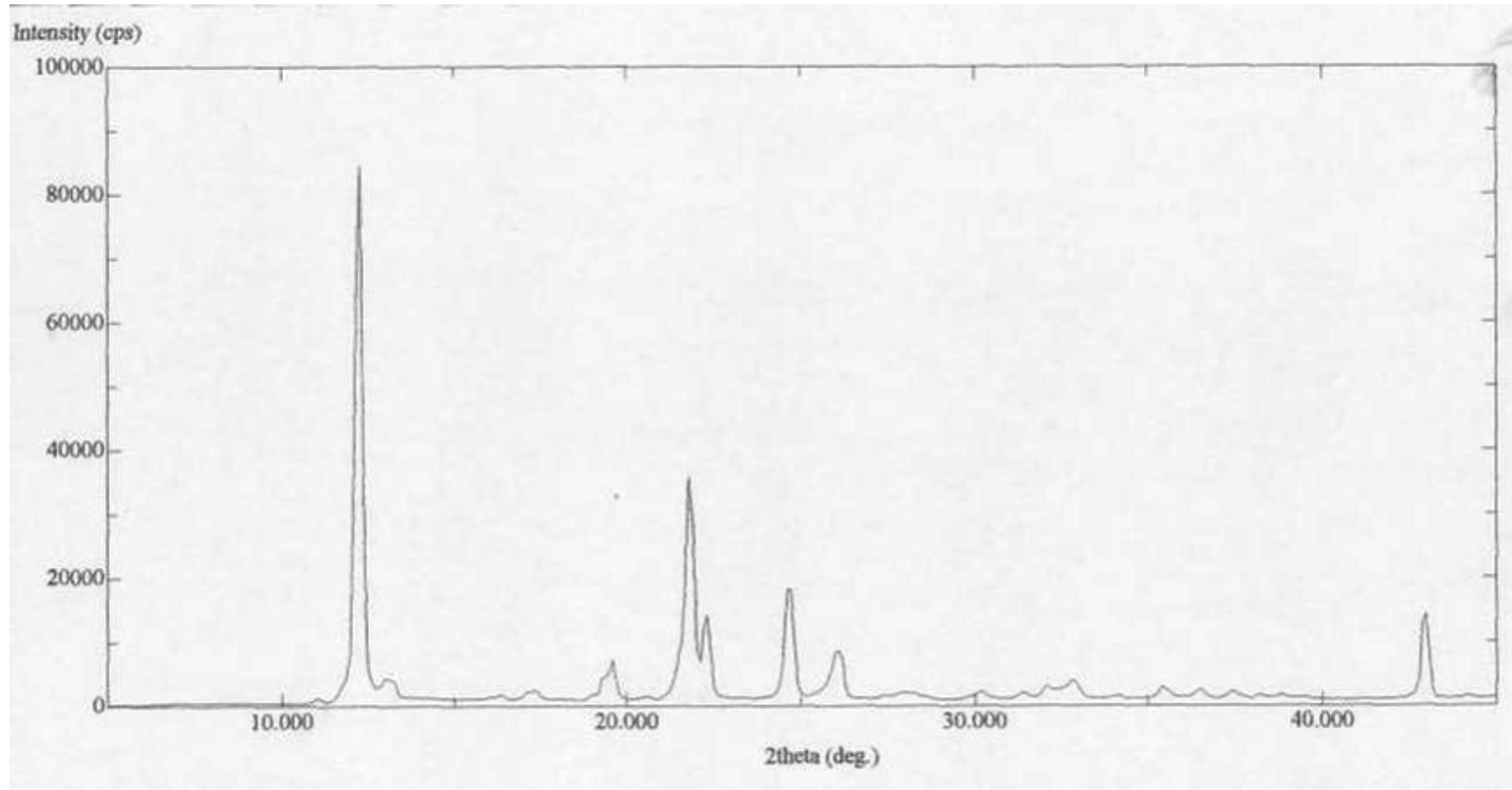**Figure 3.27 X-Ray spectrum of monomer-polymer ( 10% PVCL) mixture**

**Table 3.11 X-Ray Anaysis of monomer-polymer ( 10% PVCL) mixture**

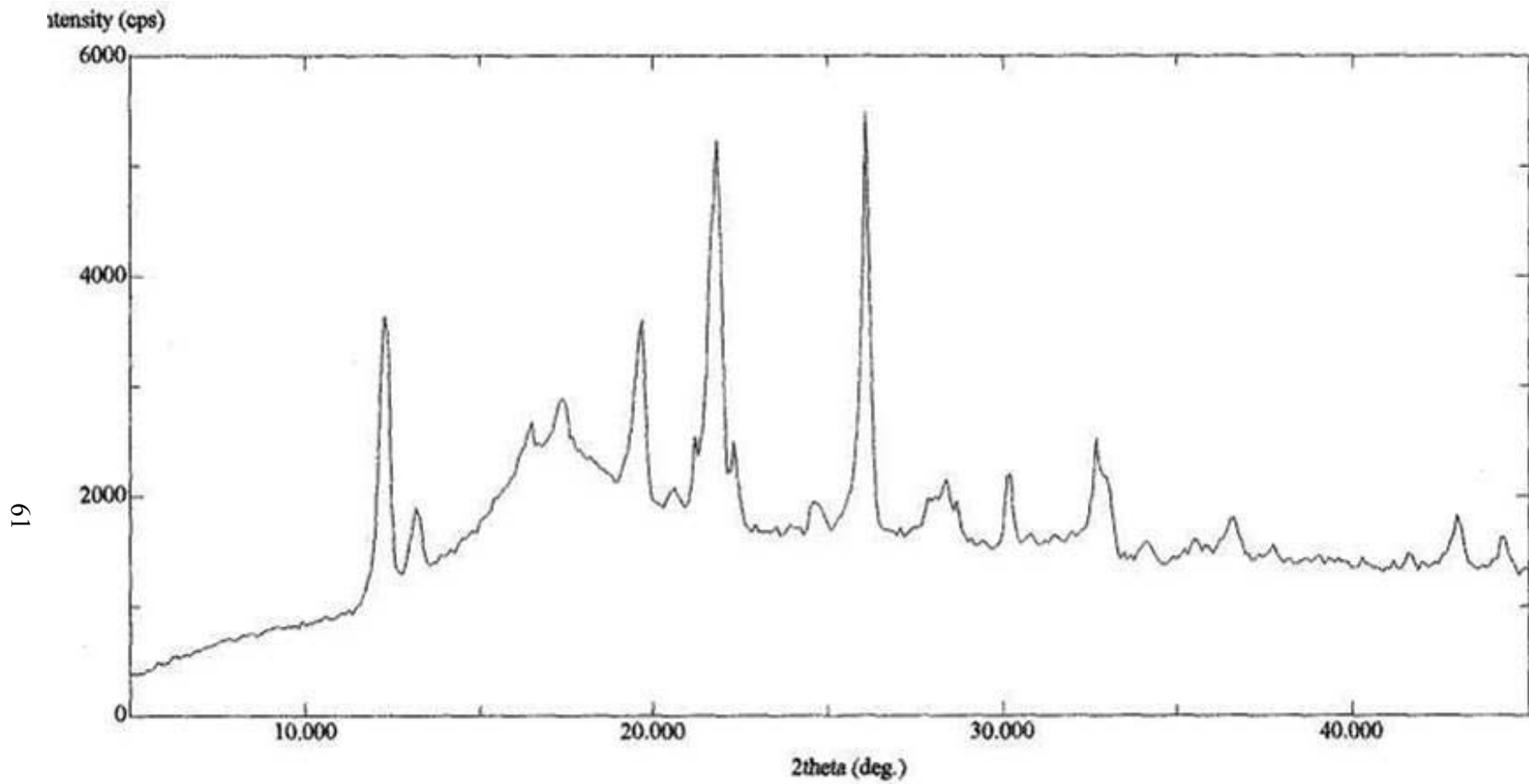| Peak no | 2θ | d-Value | Intensity | I/Io | d-calc. | h | k | l |
|---|---|---|---|---|---|---|---|---|
| 1 | 12,3 | 7,1898 | 83187 | 100 | 7,1962 | 0 | 1 | 0 |
| 2 | 13,2 | 6,7015 | 2661 | 4 | 6,6849 | 0 | 0 | 1 |
| 3 | 17,4 | 5,0922 | 1332 | 2 | 5,1096 | -1 | 0 | 1 |
| 4 | 19,6 | 4,5253 | 6183 | 8 | 4,5209 | -1 | 1 | 1 |
| 5 | 21,8 | 4,0734 | 34330 | 42 | 4,0676 | 2 | -1 | 0 |
| 6 | 22,3 | 3,9832 | 12822 | 16 | 3,9784 | 1 | -2 | 0 |
| 7 | 24,6 | 3,6157 | 16849 | 21 | 3,5981 | 0 | 2 | 0 |
| 8 | 26,1 | 3,4112 | 7236 | 9 | 3,4117 | 2 | -2 | 0 |
| 9 | 30,2 | 2,9568 | 1373 | 2 | 2,9526 | 0 | 2 | 1 |
| 10 | 31,4 | 2,8465 | 1063 | 2 | 2,8465 | -1 | -1 | 2 |
| 11 | 32,1 | 2,786 | 1867 | 3 | 2,794 | 1 | 2 | 0 |
| 12 | 32,9 | 2,72 | 2709 | 4 | 2,7191 | -2 | -1 | 1 |
| 13 | 36,5 | 2,4596 | 1443 | 2 | 2,4575 | 3 | 0 | 0 |
| 14 | 37,4 | 2,4024 | 1060 | 2 | 2,4043 | 2 | 0 | 2 |

**Figure 3.28 X-Ray spectrum of monomer-polymer (50% PVCL) mixture**

**Table 3.12 X-Ray Analysis of monomer-polymer ( 50% PVCL) mixture**

| Peak no | 2θ | d-Value | Intensity | I/Io | d-calc. | h | k | l |
|---------|------|---------|-----------|------|---------|----|----|---|
| 1 | 12,3 | 7,1898 | 3636 | 67 | 7,1962 | 0 | 1 | 0 |
| 2 | 13,2 | 6,7015 | 1893 | 35 | 6,8234 | 1 | -1 | 0 |
| 4 | 17,4 | 5,0922 | 2889 | 53 | 5,1096 | -1 | 0 | 1 |
| 5 | 19,7 | 4,5026 | 3598 | 66 | 4,5069 | 0 | 1 | 1 |
| 6 | 22,3 | 3,9832 | 2497 | 46 | 3,9784 | 1 | -2 | 0 |
| 7 | 26,1 | 3,4112 | 5484 | 100 | 3,4117 | 2 | -2 | 0 |
| 8 | 28,4 | 3,140 | 2151 | 40 | 3,148 | 2 | 0 | 1 |
| 9 | 30,2 | 2,9568 | 2199 | 41 | 2,9526 | 0 | 2 | 1 |
| 10 | 32,7 | 2,7362 | 2518 | 46 | 2,7429 | -1 | -2 | 1 |
| 11 | 33 | 2,712 | 2168 | 40 | 2,7191 | -2 | -1 | 1 |
| 12 | 34,1 | 2,627 | 1586 | 29 | 2,6284 | 2 | -1 | 2 |
| 13 | 36,6 | 2,4531 | 1801 | 33 | 2,4575 | 3 | 0 | 0 |
| 14 | 37,7 | 2,384 | 1553 | 29 | 2,3871 | -3 | 2 | 1 |
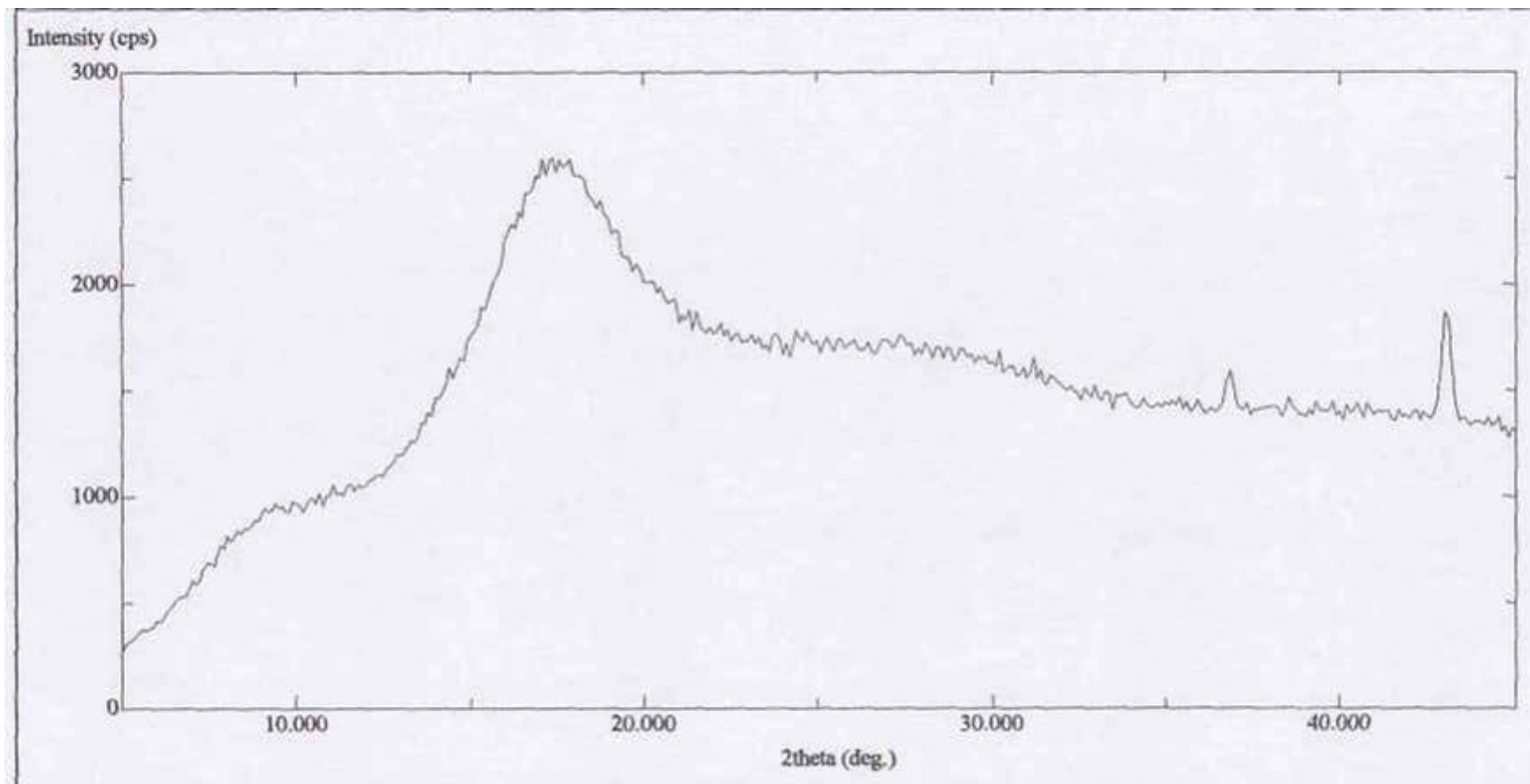
**Figure 3.29 X-Ray spectrum of monomer-polymer ( 86% PVCL) mixture**
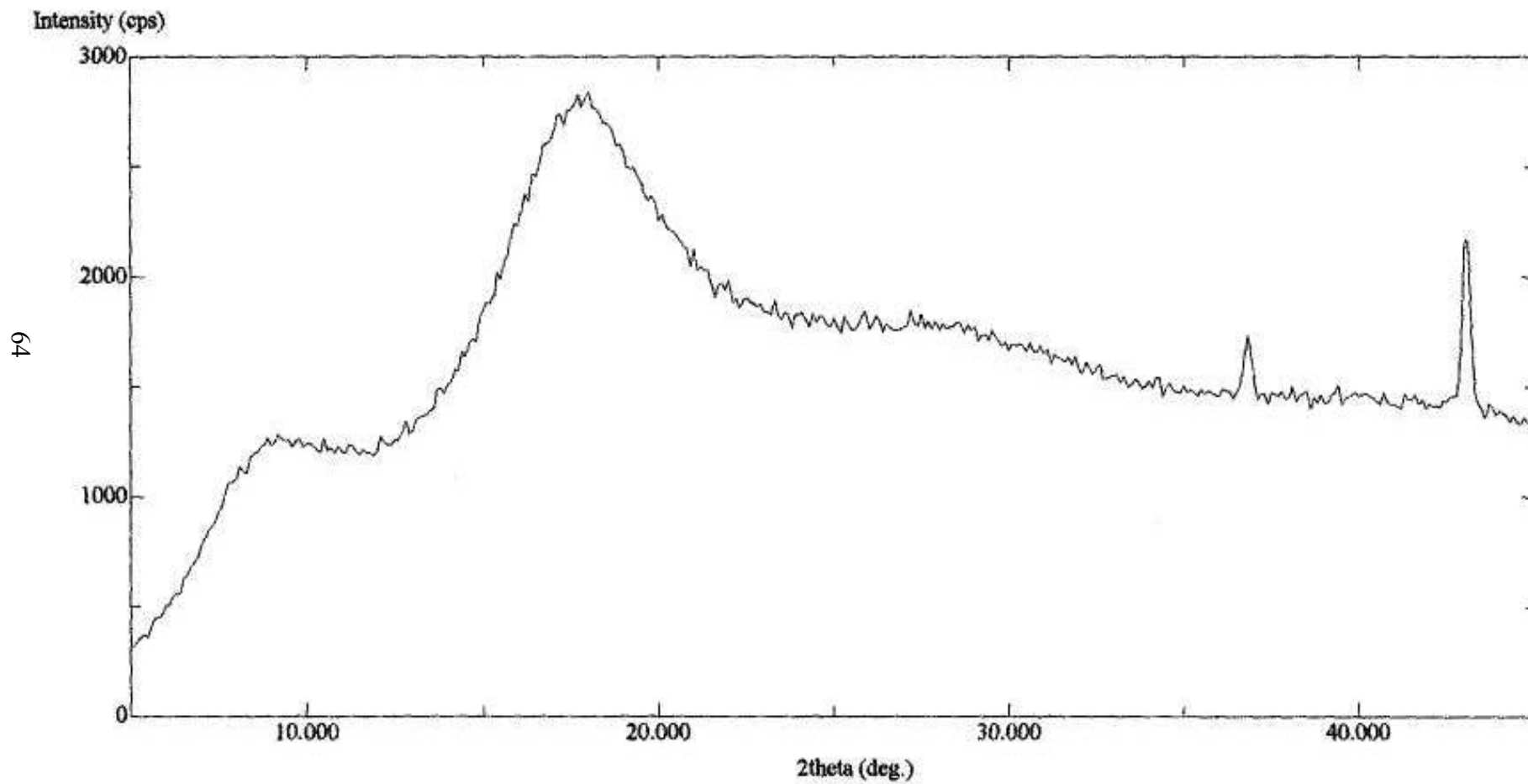
**Figure 3.30 X-Ray spectrum of PVCL**

64

## 3.8 MASS SPECTRAL ANALYSIS

The mass spectrum of the monomer is given in Figure 3.31. Monomer peak is quite intense. Yet, there are some high mass peaks indicating presence of oligomers. The base peak is at m/z=57 Da due to $N=COHCH_2$ indicating that McLafferty rearrangement reaction was the main dissociation path way during ionization. The second intense peak is at m/z=43 Da due to $N=COH$. Other intense peaks are at m/z=41,69, 71, 83 and 97 due to $C_3H_5$ ; $C_3H_6CH=CH_2$ , $CH_2=CH-N=CH_2$ ; $N=C(OH)(CH_2)_2$ ; $CH_2=CH-N(CO)(CH_2)_2$ ; $C=O(CH_2)_3CH=CH_2$ respectively. In Table 3.13 the mass spectral data is given.

In Figure 3.32 total ion-current, (TIC) curve, the variation of total ion yield as a function of temperature, and the pyrolysis mass spectra of the polymer recorded at weak and broad peak at 290 C and at the maximum of the TIC curve at 445 C are shown.

It can be observed from the figure that the main decomposition occurred above $430^0C$ in accordance with the TGA. The base peak in the mass spectrum recorded at 290 C is at m/z= 56 Da due to $(CH_2)_5$. The highest mass fragment is monomer. Evolution of water was also detected around this temperature range. At the final stage of pyrolysis the base peak was at m/z=152 Da at is due to M+CH. Yet monomer yield was also quite intense. The data indicated cleavage of side groups from the low molecular weight oligomers. Yet, it seems that the loss of side groups occurred mainly during the ionization processes inside the mass spectrometer. Thus it may be concluded that the thermal degradation occurs by random cleavages of the polymer backbone in a single yielding mainly monomer and low molecular weight oligomers. In Table 3.14 and 3.15 the mass spectral data recorded at 290 and 445 C are summarized respectively.

However, in order to be sure about the thermal degradation processes taking place the single ion pyrograms, the variation of intensity of a single product ion as a function of temperature were also studied. In Figure3.33 , the single ion pyrograms, evolution profiles of some selected products are shown. It can be observed form figure that besides $H_2O$, monomer and dissociation products the monomer, thermal decomposition mainly occured in the final stage of pyrolysis.
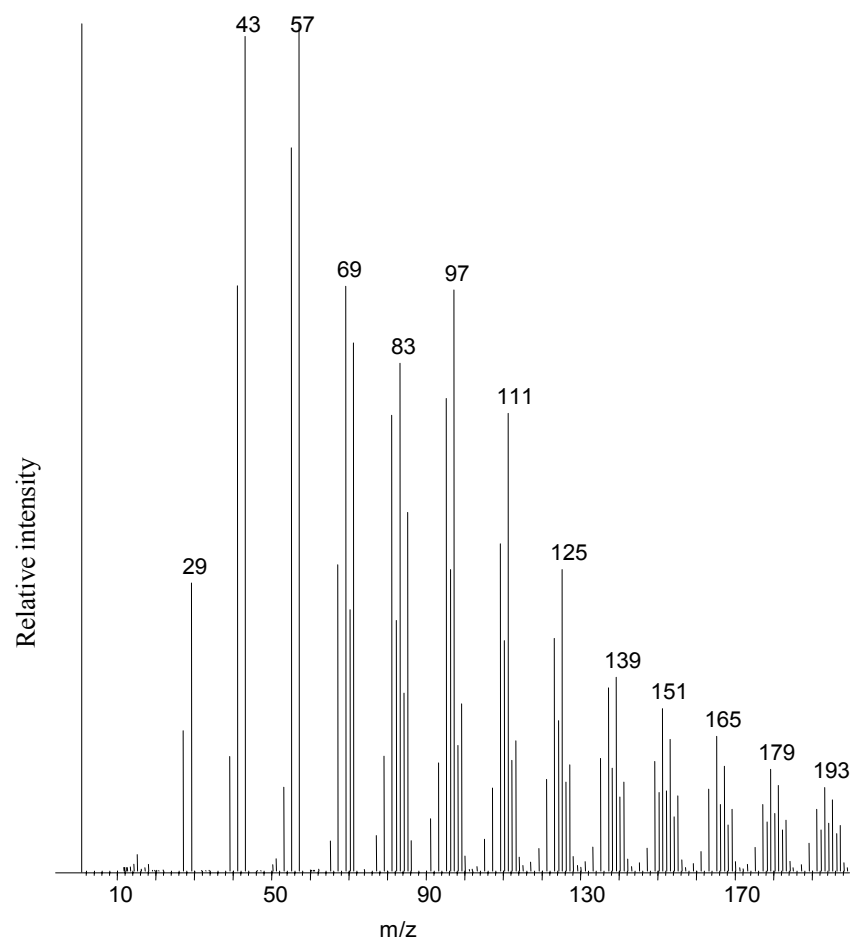
**Figure 3.31 Mass spectrum of the monomer**

**Table 3.13 The assigned fragments of monomer in mass spectrum**

| m/z | Relative Intensity | Assignment |
|---|---|---|
| 29 | 34 | COH, $C_2H_5$ |
| 41 | 69 | $C_3H_5$ |
| 43 | 98 | N=C-OH , $CH_2$=C-OH |
| 55 | 85 | $C_2H_4$-CH=$CH_2$ , $CH_2$-CH-N-$CH_2$ |
| 57 | 100 | N=C(OH)$CH_2$ |
| 69 | 69 | $C_3H_6$CH=$CH_2$ , $CH_2$=CH-N=$CH_2$ |
| 70 | 31 | $C_5H_{10}$ |
| 71 | 62 | N=C(OH)$(CH_2)_2$ |
| 83 | 60 | $CH_2$=CH-N(CO)$(CH_2)_2$ |
| 85 | 42 | N=C(OH)$(CH_2)_3$ |
| 95 | 56 | $C_5H_5NO$ |
| 97 | 69 | C=O$(CH_2)_3$CH=$CH_2$ |
| 109 | 39 | $C_7H_{11}N$ |
| 111 | 54 | M-$CH_2$-$CH_2$ |
| 125 | 36 | M-$CH_2$ |
| 139 | 23 | monomer |
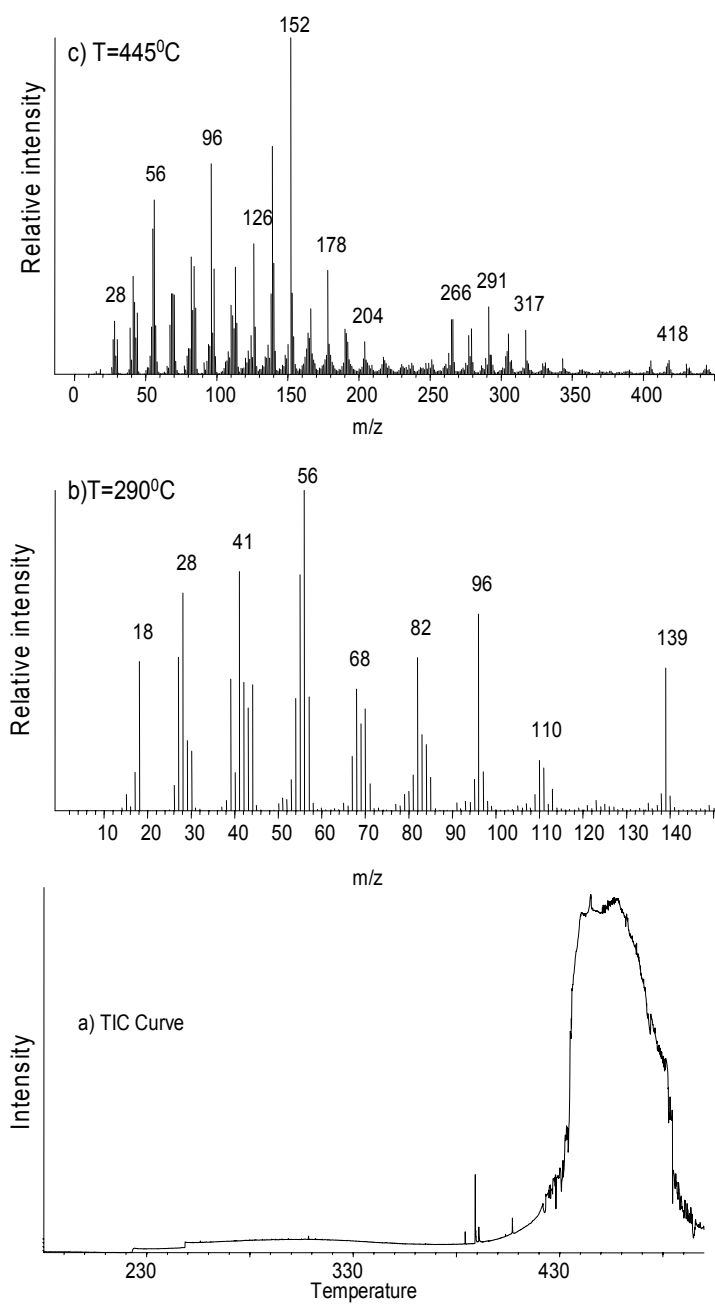
**Figure 3.32 Mass spectrum of PVCA**

69

**Table 3.14 The assigned fragments of polymer in mass spectrum at 290$^o$C**

| m/z | Relative Intensity | Assignment |
|---|---|---|
| 18 | 47 | $H_2O$ |
| 27 | 51 | $C_2H_3$ |
| 28 | 69 | $C_2H_4$ ,CO |
| 29 | 21 | COH , $C_2H_5$ |
| 30 | 21 | NO |
| 39 | 40 | $C_3H_3$ |
| 41 | 75 | $C_3H_5$ |
| 42 | 41 | $C_3H_6$ , $CH_2$=CN-N |
| 43 | 35 | NCOH , $CH_2$COH |
| 44 | 38 | $CO_2$ , $CH_2$C(OH)N |
| 54 | 33 | $C_4H_6$ |
| 55 | 75 | $C_4H_7$ |
| 56 | 100 | $NCOCH_2$ , $(CH_2)_4$ |
| 57 | 37 | $CH_2$C(OH)N |
| 68 | 38 | $C_5H_8$ |
| 69 | 26 | $C_5H_9$ |
| 70 | 31 | $C_5H_{10}$ |
| 82 | 49 | $CH_2$=CH-$CH_2$-CH-N=$CH_2$ |
| 83 | 27 | $CH_2$=CH$(CH_2)_2$CO |
| 84 | 21 | $(CH_2)_4$CO |
| 96 | 58 | M-($CH_2$COH) |
| 97 | 14 | C=O$(CH_2)_3$CH=$CH_2$ |
| 139 | 47 | monomer |

**Table 3.15 The assigned fragments of polymer in mass spectrum at 445°C**

| m/z | Relative Intensity | Assignment |
|-----|--------------------|------------|
| 28 | 16 | $C_2H_4$ , CO |
| 41 | 29 | $C_3H_5$ |
| 42 | 21 | $C_3H_6$ , $CH_2=CH-N$ |
| 44 | 18 | $CO_2$ , $CH_2C(OH)N$ |
| 55 | 43 | $C_4H_7$ |
| 56 | 52 | $NCO(CH_2)$ , $(CH_2)_4$ |
| 68 | 24 | $C_5H_8$ |
| 69 | 24 | $CH_2=CHN(CH_2)_2$ , $C_5H_9$ |
| 70 | 24 | $C_5H_{10}$ |
| 82 | 35 | $CH_2=CH-CH_2-CH-N=CH_2$ |
| 83 | 19 | $CH_2=CH(CH_2)_2CO$ |
| 84 | 32 | $(CH_2)_4CO$ |
| 96 | 63 | $M-(CH_2COH)$ |
| 97 | 12 | $CH_2=CH-NCO(CH_2)_4$ |
| 98 | 31 | $CH_2CH-NCOH(CH_2)_2$ |
| 112 | 14 | $CH_2=CH-NCOCH_2$ |
| 126 | 39 | $CH_2CH-NCOH(CH_2)_4$ |
| 138 | 24 | M-H |
| 139 | 68 | Monomer |
| 152 | 100 | M+CH |
| 166 | 20 | $MCH_2=CH$ |
| 178 | 31 | $M-CH_2=CHCH_2$ |
| 279 | 13 | DH |
| 305 | 12 | $DCH=CH_2$ |
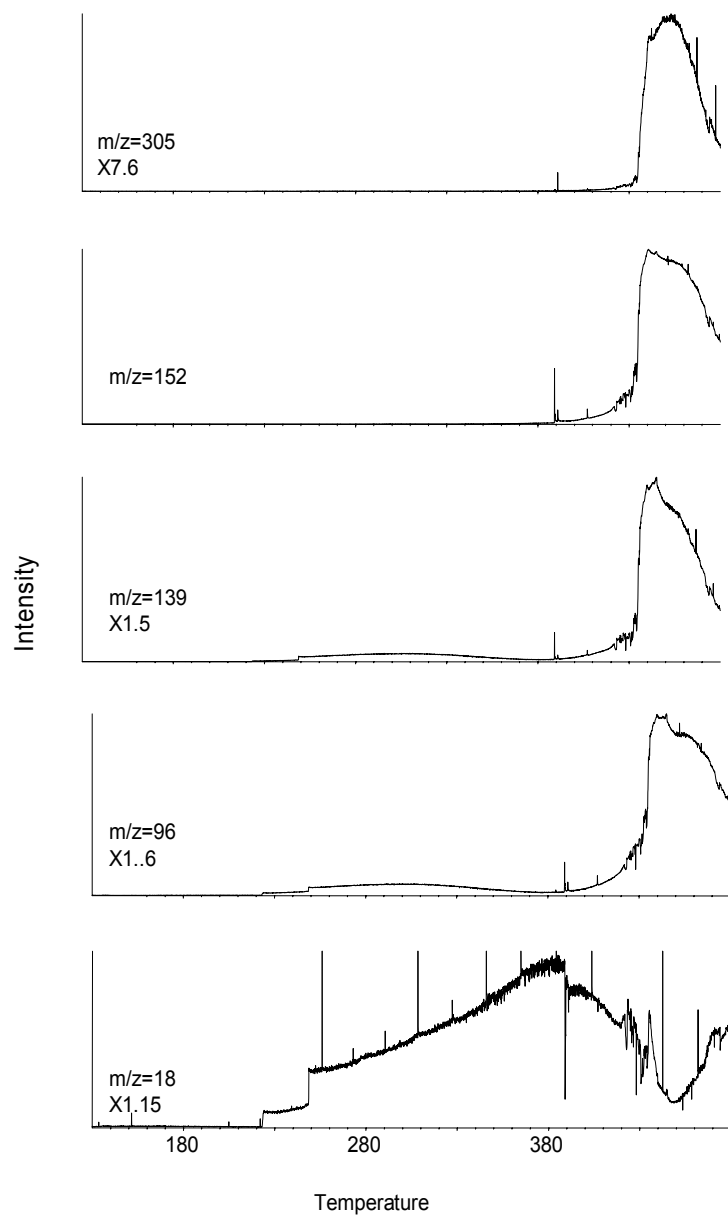
**Figure 3.33 The single ion pyrograms in selected products**

72

# CHAPTER IV

## CONCLUSION

In this study, N-vinylcaprolactam was polymerized in solid state by radiation. Polymerization was carried out in vacuum and in open atmosphere at room temperature. The following conclusion were derived from this study:

1. The rate of polymerization was higher in open air and limiting conversion was 100% in vacuum; 90% in open atmosphere.
2. Polymer obtain was gel type soluble in water and most common organic solvents.
3. FT-IR and NMR results show that polymerization proceeded by opening of vinyl group.
4. The light scattering, GPC and viscosity methods useful for molecular weight determination showed that the polymer conformation in solution highly dependent on molecular weight. Therefore, a simple relation between intrinsic viscosity and molecular weight could not be obtained.
5. X-Ray structure determination showed that the cyristal structure of monomer retained its identity up to about 86% conversion. The polymer was amorphous but showed some polymer chain regularity and chain orientation up to a certain extend.
6. Mass spectrum analysis of monomer and polymer gave the fragments compatible with a vinyl group backbone chain and lactam as side group.

# REFERENCES

1.  Charlesby, A., Atomic Radiation and Polymers, Pergamon Press, Newyork, (1960)

2.  Ivanov, V. S., Radiation Chemistry of Polymers, Utrecht, The Netherlands, (1992)

3.  Schmitz, J.V. and Lawton, E.J., Sciences, 113, 718, (1951)

4.  Adler, G., Ballantine, D.S., and Baysal B., J.of Polym.Sci., 48, 198, (1954)

5.  Restaiona, A.J., Mesrobian, R.B., Morawetz, H., Ballatine, D.S., Dienes, G.J. and Metz, D.J, J.A.Chem. Soc., 78,2939, (1956)

6.  Lawton, E.J. Grubb, W.T. and Balwit, J.S., J.S., J.Polymer sci., 19, 455, (1956)

7.  Morowetz, H. and Rubin, I.D., J.Polym.Sci., 57, 669, (1962)

8.  Lando, J. B., Morowetz H., I.D., J. Polymer Sci., C4, 789, (1963)

9.  Charlesby, C. A., Morris, J., Proc. Roy. Soc.A., 281, 392, (1964)

10. Adler, G. and Reams, W., J. Chem.Phys., 32, 1698, (1960)

11. Adler , G., Ballantine, D.S. and Baysal, B., J. Polym. Sci., 48, 195, (1960)

12. Usanmaz, A., Turk. J. Chem.,21, 304-312, (1997)

13. Bamford, C.H., Eastmond, G.C. and Ward, G.C., Proc. Roy. Soc. (London), 271, 357, (1967)

14. Bunn, C.W., Nature, 161, 929, (1948)

15. Natta, G. and Carradini, P., J. Polym. Sci., 20,251, (1956)

16. Natta, G., Carradini, P. And Allegra, G., Atti. Acad. Naz. Lincei, Rend., 31, 350, (1961)

17. Hayashi, K., Isotopes and Radiation 3, 416, (1960)

18. Hayashi, K., Isotopes and Radiation 3, 510, (1960)

19. Hayashi, K., Isotopes and Radiation 3, 346, (1960)

20. Hasegawa, M. And Suzuki, Y.Y ., J. Polym. Sci., B-5, 813, (1967)

21. Usanmaz, A., and Melad, O.K., J.Polym.Sci., Part A., Polym. Chem., 34, 1087, (1996)

22. Masayuki, A., J. of Applied Polym. Sci., 33, 1793-1807 (1987)

23. Usanmaz, A. and Yılmaz, E.,J. Macromol., Sci- Chem., A-24(5), 479-491, (1987)

24. Nasimova, I. R., Evlanova, Makhaeva, E. E.,Khokhlov, A. R., Journal of Applied Polymer Science, 81, 12, 2838-2842, (2001)

25. Tishchenko, G. N., Zhukhlistova, N. E., Kirsh, Yu. E., Crystallography Reports, 42, 4, 626-630, (1997)

26. Kirsh,Yu. E., Yanul, N. A., Kalninsh, K. K.,European Polymer Journal, 35, 305-316, (1999)

27. Andy, C.W., Lau, C.W., Macromolecules., 32, 581, (1999)

28. Laukkanen, A., Ph.D. Thesis, University of Helsinki, (2005)

29. Cheng, S. C., Feng, W., Pashikin, I.I., Yuan, L. H., Deng, H. C., Zhou, Y., Radiation Physics and Chemistry, 63, 517-519, (2002)

30. Lozinsky, V. I., Simenel, I. A., Kurskaya, E. A., Kulakova, V. K., Galaev, I. Yu., Mattiasson, B., Grinberg, V. Ya., Grinberg, N. V., Khokhlov, A. R., Polymer, 41, 6507-6518, (2000)

31. Gao, Y., Steve, C. F., Au-Yeung, Chi Wu, Macromolecules, 32, 3674-3677, (1999)

32. Morgret, L. D., Hinkley, J. A., NASA/TM-2004-212992, (2004)

33. Peng, S., Chi Wu, J. Phys. Chem. B ,105, 2331-2335, (2001)

34. Ivanov, A. E., Kazakov, S. V., Galaev, I. Yu., Mattiasson, B., Polymer, 42, 3373-3381, (2001)

35. Solomon, O. F., Corciovei, M., Ciuta, I., Boghina, C., J. Appl. Pol. Sci. 12(8), 1835, (1968)

36. Anufrieva, E. V., Gromova, R. A., Kirsh, Yu. E., Yanul, N. A., Krakovyak, M. G., Lushchik, V. B., Pautov, V. D., Sheveleva, T. V., Eur. Polym. J. 37 323-328, (2001)

37. Kudryavtsev, Val. N., Kabanov, V. Ya., Yanul, N. A., Kedik, S. A., Radiation Chemistry, 37, 6, 382-388, (2003)

38. Mamytbekov, G., Bouchal, K., Ilavsky, M., Eur. Polym. J., 35, 1925-1933, (1999)

39. Makhaeva, E. E., Tenhu, H., Khokhlov, A. R., Polymer, 41, 9139-9145, (2000)

40. Lebedev, V. T., Török, Gy., Cser, L., Kali, Gy., Kirsh, Yu. E., Sibilev, A. I., Orlava, D. N., Physica B, 297, 50-54, (2001)

41. Alexander, Leroy E., X-Ray Diffraction Methods in Polymer Science New York, Wiley –Interscience, (1969)

42. Ghassempour, A., Najafi, N. M., Amiri, A. A., J. Anal. Appl. Pyrolysis, 70, 251-261, (2003)

43. Radovic, B. S., Goodacre, R., Anklam, E., J. Anal. Appl. Pyrolysis, 60, 79-87, (2001)

44. Fazlıoglu, H., Hacaloglu, J., J. Anal. Appl. Pyrolysis, 63, 327-338, (2002)

45. Gozet, T., Onal, A. M., Hacaloglu, J., Synthetic Metals, 135-136, 453-454, (2003)

46. Badawy, S. M., Radiation Physics and Chemistry, 61, 143-148, (2001)